J. Fluid Mech. (2008), *vol.* 602, *pp.* 81–117.
doi:10.1017/S0022112008000724 Printed in the United Kingdom

Normal-mode linear analysis and initial conditions of capillary jets

F. J. GARCÍA[1,3] AND H. GONZÁLEZ[2,3]

[1]Departamento de Física Aplicada I, Escuela Técnica Superior de Ingeniería Informática, Universidad de Sevilla, Avenida Reina Mercedes s/n, 41012 Sevilla, Spain

[2]Departamento de Física Aplicada III, Escuela Técnica Superior de Ingenieros, Universidad de Sevilla, Camino de los Descubrimientos s/n, 41092 Sevilla, Spain

[3]Group of Electrohydrodynamics and Cohesive Granular Media, Facultad de Física, Universidad de Sevilla, Avenida Reina Mercedes s/n, 41012 Sevilla, Spain

(Received 30 March 2007 and in revised form 17 January 2008)

The normal-mode linear analysis of an axisymmetric infinite capillary jet is generalized to account for arbitrary initial conditions. An exhaustive study of the dispersion relation reveals the parametric behaviour of all eigenvalues and their corresponding normal modes. The two capillary modes (dominant and subdominant) are found to be necessary and sufficient to describe any possible non-recirculating initial conditions. An infinite set of other modes accounts for initial conditions with recirculating velocity field. The predictions of the normal-mode analysis are contrasted against previous computations of the initial-value problem, previous experiments, and our own one-dimensional numerical simulations. Contrary to the claim of some authors, the normal-mode analysis accurately predicts the initial transient with non-exponential growth of the disturbance amplitude observed in previous works. Simple and accurate formulae for the duration of the initial transient are deduced, with emphasis on improving the growth-rate measurement.

1. Introduction

A capillary jet forms when a liquid emanates from a usually circular hole rapidly enough to avoid dripping. It is well known, however, that the resulting liquid column cannot conserve its initial cylindrical shape: any infinitesimal perturbation, either noisy or controlled, with wavelength beyond a critical value destabilizes the system. The perturbation grows up and finally leads the jet to break up downstream into drops. With an appropriate initial disturbance, this is an efficient way to produce small droplets of controlled size. Since the pioneering work of Plateau (1873) and Rayleigh (1945), we know that the surface-tension force is responsible for this instability, as the adjective *capillary* announces. Thus, the system naturally evolves to decrease its free surface. However, they also noticed that inertia and viscous stresses are important to explain the growth of disturbances.

The potential technological applications of capillary jets has attracted the interest of many workers. After the first electrostatically deflected ink-jet device of Sweet (1965), the early development of ink-jet printing technology catalysed a considerable effort in the 1970s, both theoretical and experimental (see Le 1998, for a description of techniques). This technology rapidly propagated to other fields of invention that required both rapid and accurate formation and positioning of small droplets.

Nowadays, it is successfully used in flow cytometry and cell sorting (Shapiro 2003). Liquid jets are also valuable as targets for high-power laser-plasma generators of ultraviolet and X-rays (Hansson & Hertz 2004). See Basaran (2002) for a detailed review of applications.

Temporal analysis has been the most widely employed approach to predicting the evolution of capillary jets. The jet is assumed to be an infinitely long cylindrical liquid column subjected to periodic initial perturbations of its surface. This so-called *infinite jet* tries to approximate the real jet emerging from a nozzle, often referred to as the *semi-infinite* jet. The infinite jet is a simpler system: the spatial domain of the infinite jet can be reduced to a small length (the wavelength of the perturbation), and boundary conditions are simply periodic. In contrast, the semi-infinite jet cannot be considered strictly periodic; the spatial domain is the whole length of the jet; and the additional boundary conditions at the orifice and downstream hinder the analysis. The semi-infinite jet treatment can be formally recovered from temporal analysis through a simple Galilean transformation, provided the jet velocity is large enough, relative to the capillary velocity (Keller, Rubinow & Tu 1973). This happens in many practical situations.

Even in the infinite-jet approximation, solving the resulting time-dependent free-boundary problem with nonlinear three-dimensional equations is a formidable task, fully achievable only with the aid of costly numerical methods. *Linear temporal analysis* was the first analytical attempt to solve it (Rayleigh 1878, 1892). This first-order perturbative analysis considers small-amplitude perturbations of a static infinite cylinder. The resulting set of equations and boundary conditions is linear and the spatial domain is fixed (a cylinder).

Instead of trying to solve this linear problem directly for any arbitrary perturbation, the classical approach consists in expressing the solution as a superposition of Fourier modes, each of these having an appropriate sinusoidal dependence on both the axial and azimuthal coordinates. This allows us to separate the temporal and radial dependence of pressure, velocity and surface deformation. The radial dependence is found by imposing the radial boundary conditions. The remaining problem is a linear initial-value problem for the time dependence of each Fourier mode, characterized by a non-negative integer azimuthal number m and a real positive axial wavenumber k. When perturbations are axially periodic, as is usual in controlled stimulation, the wavenumber spectrum is finite and the actual solution can be formally expressed as an infinite discrete sum of these modes: a fundamental and its harmonics. When they are not periodic, as happens with natural noisy perturbations, such a spectrum is continuous, and an integral in k replaces the sum. At this point, two possible approaches for finding the time dependence of pressure, velocity and surface deformation have been considered in the literature: the Rayleigh normal-mode analysis and the initial-value problem.

The often-called *Rayleigh normal-mode analysis* assumes a solution with a complex exponential dependence on time, $\exp(\hat{\alpha}t)$, instead of choosing a particular set of initial conditions. Substituted into the linear ordinary differential equation for the time dependence of the Fourier mode, a dispersion relation is found, which relates the complex eigenvalue $\hat{\alpha}$ to m, k and the parameters of the fluid. Each root $\hat{\alpha}$ of the dispersion relation is associated with an eigenfunction for pressure, velocity and surface deformation: a normal mode of the infinite jet. The real part of the eigenvalue, $\alpha = \mathrm{Re}(\hat{\alpha})$, gives the growth rate; while the imaginary part $\omega = \mathrm{Im}(\hat{\alpha})$ gives the oscillation frequency of the normal mode. The growth rate is positive only for axisymmetric perturbations ($m = 0$) with wavenumber smaller than the inverse of

the radius of the unperturbed jet, the so-called *Plateau cutoff wavenumber*, or simply *cutoff wavenumber*.

Many authors discuss the problem directly in terms of these normal modes, without discussing explicitly the initial conditions. This is because the modes with greater positive growth rate, the most meaningful, rapidly dominate over the other. Therefore, monoharmonic initial conditions are expected to degenerate in a Rayleigh dominant mode with exponential growth of both velocity and surface disturbance. In fact, the terms 'Fourier mode' and 'normal mode' are usually thought to be equivalent. This has led to a commonly accepted assumption: the normal-mode analysis predicts a purely exponential growth of the amplitude of a monoharmonic initial disturbance. Suspecting a possible role of specific initial conditions, several authors have solved the initial-value problem for the temporal dependence of the perturbative analysis. Most of them chose inviscid liquids and simple initial conditions: either an initially static deformation or the more realistic pure impulse with no deformation. Berger (1988) solved the initial-value problem for arbitrary viscosity and mixed initial conditions. This approach showed an initial departure from the purely exponential growth expected from the Rayleigh normal-mode analysis. Most authors had disregarded this transient. Berger noticed that it depends on the actual initial conditions. He claimed that the Rayleigh normal-mode analysis is both formally and practically wrong. Since then, other authors have noticed this initial transient when solving initial-value problems numerically and have cited Berger's arguments against the normal-mode analysis. However, as Berger's formalism is hard to implement, no predictions about the initial transient form and duration have been made available up to now.

This paper is concerned with the predictive power of the Rayleigh normal-mode analysis of a capillary jet. Contrary to Berger's claim, we shall show that the initial transient can be seen as a direct consequence of the relation between the initial conditions and the Rayleigh normal modes. It will be evident how important it is to know the physical origin and parametric behaviour of all normal modes. Some of them, generally ignored, will allow us to estimate how long a recirculating perturbation takes to damp. Our analysis will provide simple and accurate formulae for the amplitude evolution under general initial conditions, as well as the transient duration for pure-deformation and pure-impulse initial conditions. We shall explain how the initial transient introduces systematic errors when measuring the growth rate; and how to avoid these errors, either in experiments or in computations. The accuracy of the normal-mode analysis will be contrasted with the aid of previous results and our own numerical simulations.

Owing to the basic nature of the subject, there are many previous results relevant to our discussion. In order to fit all the pieces of this puzzle into the framework of the normal-mode linear analysis, the previous work is reviewed in the next section. Afterwards, the modal analysis of Rayleigh and Chandrasekhar is extended to consider all normal modes and its relation to the initial conditions. We then present some results from this modal linear analysis and from a nonlinear one-dimensional model. Next, these results and previous ones in the literature are discussed. Finally, the main conclusions are drawn.

2. Previous work

We do not intend to rigorously examine all previous literature on capillary jets. Eggers (1997) gives a general view and pending challenges; Lin (2003) is a more recent source of bibliography.

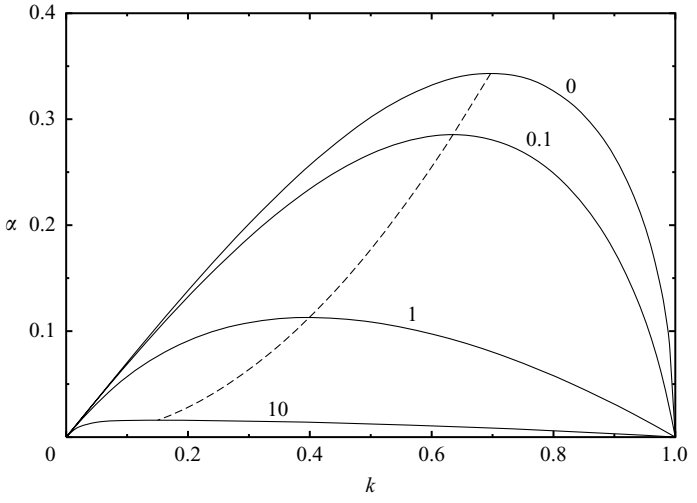

FIGURE 1. Non-dimensional growth rate α of the most significant mode versus non-dimensional wavenumber k (perimeter of the jet cross-section divided by the wavelength), for the labelled non-dimensional Ohnesorge numbers C (viscous stresses relative to capillary pressure). The dashed line shows how both α_{max} and its corresponding wavenumber k_{max} decrease as C increases.

2.1. *Rayleigh dispersion relation*

Rayleigh carried out the modal analysis of the viscous infinite jet (Rayleigh 1892). Although he formally deduced the corresponding dispersion relation for any possible viscosity, he could analytically solve it only for zero and paramount viscosity (Rayleigh 1878, 1892). It was Chandrasekhar (1961) who obtained numerical solutions for non-zero finite viscosity. Their results show that positive growth rates are found only for axisymmetric perturbations ($m = 0$) with wavelength greater than the perimeter of the cross-section of the original cylinder, a limit predicted by Plateau (1873). This is why axisymmetric long-wavelength modes are the most commonly considered in the literature, while those with negative growth rate are often ignored.

Figure 1 condenses the general understanding of the Rayleigh three-dimensional modal temporal analysis (Rayleigh 1878; Chandrasekhar 1961). The greater the growth rate is, the more significant the mode is. This makes specially important the modes with the greatest growth rate, α_{max}; with a non-dimensional wavenumber k_{max}. For inviscid liquids, $k_{max} = 0.697$, diminishing as viscosity increases.

It is known that, besides the solution depicted above, there are more solutions to the dispersion relation, but with non-positive growth rates. Rayleigh (1878) found them for inviscid liquids; and so did Weber (1931) for viscous liquids, with a linear one-dimensional analysis. However, the corresponding decaying modes are generally ignored in favour of the growing dominant modes. Remarkably, Grossmann & Müller (1984) found more eigenvalues of the dispersion relation in their linear analysis of charged jets. Besides the two normal modes mentioned, they identified an infinite set of other modes, all of them decaying, with recirculating velocity field. Apparently, this fact has remained unnoticed, with the exception of García (1998). Nicolás & Vega (2000) found a similar set of modes in their three-dimensional linear analysis of a viscous liquid bridge.

The estimate of the breakup time and the breakup length of the jet is one of the most important results of the linear analysis. Breakup arrives when the deformation

amplitude becomes the radius of the jet. If exponential growth of the initial deformation is assumed, the breakup time can be estimated by

$$t_b = \frac{-\ln(\tilde{f}_0)}{\alpha}, \tag{2.1}$$

where $\tilde{f}_0$ is the initial amplitude of the sinusoidal deformation relative to the radius of the unperturbed jet (Rayleigh 1945). The breakup length of the jet emanating from a nozzle comes from multiplying t_b by the jet velocity. The greater the initial perturbation is, the smaller the breakup time and the breakup length are.

Levich (1962) alternatively defined the breakup time as the inverse of the growth rate, which is the time that the perturbation takes to grow up in a factor e. This estimate is wrong, since it omits the obvious role of the initial amplitude of the perturbation. Berger (1988) used it to claim that the initial amplitude was 'immaterial' in his comparison of experimental breakup times against his theoretical predictions.

2.2. *Initial conditions and transient phase*

Rayleigh (1878, 1892) did not consider any concrete initial conditions for capillary jets. An alternative to the Rayleigh modal analysis is to solve an initial-value problem for some explicitly given initial conditions. Yuen (1968) was the first to apply this approach to an inviscid infinite jet with zero initial velocity and a small sinusoidal deformation of the surface (hereinafter referred to as *pure-deformation* initial conditions) in his third-order perturbation analysis of inviscid jets. In practice, the initial conditions are inherited from the stimulation mechanism of the jet, which is usually acoustic. When the real jet exits from the nozzle, it is expected to be almost cylindrical, while the perturbation of pressure within the nozzle produces a perturbation of velocity outside. The first to consider an initially cylindrical infinite jet with a velocity modulation (hereinafter referred to as *pure-impulse* initial conditions) was Lee (1974), with a linear one-dimensional approach. He demonstrated its equivalence with a perturbation in pressure. Chaudhary & Redekopp (1980) applied the same initial conditions to revisit the third-order perturbation analysis of Yuen. We emphasize that all of the above initial-value problems were for inviscid liquids, and all of them found a similar time dependence, in terms of hyperbolic functions. Therefore, the corresponding estimates for the breakup time analogous to (2.1) have an inverse hyperbolic function of the initial amplitude of the perturbation, instead of a logarithm (Lee 1974).

Bogy (1978) revisited the initial-value problem of pure-impulse initial conditions stated by Lee (1974). He extended it to viscous jets with the aid of the one-dimensional Cosserat model proposed by Green (1976). It is noteworthy that the time dependence of his solution is a linear combination of two exponentials – one of them increasing with time, the other one decreasing – corresponding to the two roots of his dispersion relation. However, no physical consequences have been derived from that solution and it seems to have fallen into oblivion. Unaware of the work of Bogy, both Furlani (2005) and Chakraborty (2005) applied a similar two-normal-mode one-dimensional analysis to study the temporal instability of a viscous jet initially static and undeformed, but with spatially varying surface tension. Again, it is remarkable how such a combination of two exponentials allows us to relate the temporal evolution to the initial conditions.

The first to solve an initial-value temporal analysis for a viscous jet subjected to mixed initial conditions was Berger (1988). As in the Rayleigh modal analysis, he considered a sinusoidal axial dependence of the dependent variables. Using the

Laplace transform, he formally solved the problem, but the difficulty of the expressions compelled him to invert it numerically. In order to fit breakup times from previous drop-on-demand experiments, *ad hoc* initial conditions were chosen.

A logarithmic scale is usually chosen for the amplitude of a wave disturbance when representing its evolution in time. In this way, a typical exponential growth is represented by a straight line, whose positive slope is proportional to the growth rate. A deviation from the exponential growth is easy to detect in plots like these. This is how Berger showed that there is an initial transient phase along which the perturbation grows more slowly than in the subsequent exponential-growth phase. In his opinion, the Rayleigh mode analysis implicitly ignores this initial growth phase of the disturbance. Furthermore, he claimed that, although a discrete superposition of many modes could be proposed as a solution for describing this transient time, this is not formally permissible, because the spectrum of the disturbances is continuous. His fitted prediction apparently agrees better than his modal analysis predictions with the mentioned experiments in some parametric range.

The involved mathematical method implemented by Berger is correct. He had the merit of emphasizing the existence of an initial transient phase, before the classical exponential growth of disturbances is reached, its relation to the specific initial conditions, and its possible influence on the breakup time. However, there are a number of subtleties that we enumerate next.

(i) The system treated by him was an infinite jet with periodic initial conditions. Therefore, the Fourier spectrum is not expected to be continuous, as he claimed, but discrete.

(ii) Following Levich (1962), Berger computed the breakup time t_b as the inverse of the growth rate, which is the time that the perturbation takes to grow up in a factor e. This definition and his claim that t_b does not depend on the initial amplitude of the perturbation are wrong, as (2.1) establishes.

(iii) From a formal point of view, his initial conditions are not as general as claimed. Neither temporal phase between deformation and velocity nor recirculating initial patterns were considered.

(iv) His *ad hoc* numerical choice for the initial conditions is quantitatively unrealistic. When they are compared to the given scales and parameters of the fluid, we find that its initial velocity is 9×10^{-3} times the capillary velocity; and its disturbance amplitude is 394 times the radius of the unperturbed jet. As pointed out by Ashgriz & Mashayek (1995), this amplitude is unlikely to be found in real jets.

(v) Moreover, such almost-pure-deformation initial conditions are qualitatively unrealistic, because real jets usually have pure-impulse initial conditions. In fact, the slow-growth transient depicted by him goes against experimental evidence, as we discuss below.

(vi) The drop-on-demand technique is not appropriate to validate experimentally either a temporal or a linear theory, because the streams so generated are essentially semi-infinite and nonlinear in nature (Le 1998). The term 'drop-on-demand jet' itself is confusing, since the drop-on-demand technique does not actually produce jets, but drops.

(vii) A complete modal analysis, as the one shown in this paper, is equivalent to Berger's formalism. It takes account of arbitrary initial conditions for velocity and surface deformation; it also predicts the existence of non-exponential initial growth; but is much simpler, instructive and predictive.

Berger's numerical approach is much more involved than Rayleigh's. Thus, it is difficult to make predictions from it. In fact, it has not been used by any other

author. Even his comparison with experiments and his modal analysis are spurious, as reasoned above.

The existence of an initial non-exponential transient phase (hereinafter referred to as *initial transient*) can be visualized by representing the evolution of either the logarithmic amplitude of the surface deformation or the instantaneous growth rate. Those initial transients are evident in the figures of several authors; obtained either by perturbation analysis (Taub 1976; Chaudhary & Redekopp 1980; Berger 1988), through the numerical solution of nonlinear three-dimensional or one-dimensional equations (Bousfield & Denn 1987; Torpey 1989; Sellens 1992; Ashgriz & Mashayek 1995; Saroka, Guo & Ashgriz 2001; Collantes, Yariv & Frankel 2003; Chuech & Yan 2006; Suryo, Doshi & Basaran 2006), or experimentally (Torpey 1989; Xing *et al.* 1996). This is summarized in table 1. Two kinds of transient are found in different situations, according to the growth of the amplitude of deformation with respect to the expected exponential growth: a slow-growth transient and a rapid-growth transient. In a *slow-growth transient*, the instantaneous growth rate is initially smaller than expected; in a *rapid-growth transient*, the instantaneous growth rate is initially greater than expected. In both cases, the instantaneous growth rate tends to the value expected from the classical Rayleigh analysis after a time that characterizes the transient duration. The word 'normal' in table 1 means that there seems to be no initial transient, i.e. the growth is exponential from the beginning. References in table 1 are ordered according to the qualitative growth of the deformation during the observed transients.

Only a few short comments have been made to explain the existence and nature of these transients. Bousfield & Denn (1987), through numerical computations for pure-impulse initial conditions, found a rapid-growth transient, not predicted by their linear modal analysis. They associated the transient with a regime dominated by the balance between inertia and viscous stresses, while capillarity and viscous stresses dominate over inertia in the exponential-growth phase. Although not general, their scale argument is true for their high-viscosity example. Berger (1988) noticed that his slow-growth transient lasted longer for larger wavenumbers. Ashgriz & Mashayek (1995) numerically found a slow-growth transient for pure-deformation initial conditions and small viscosity. Noting the parallelism with Berger's results and citing him, they associated the transient with the initial presence of higher-order harmonics, which would be damped and disappear as the exponential-growth was achieved. However, their study of the temporal evolution of Fourier modes showed that the amplitudes of harmonics are negligible during the transient. For very viscous liquids, their figures show an exponential growth from the beginning. They attributed it to a rapid damping of such harmonics, but no transient could be appreciated. Chuech & Yan (2006) noticed a slow-growth transient when solving numerically a nonlinear one-dimensional model for inviscid jets with pure-deformation initial conditions. Although they computed a global growth rate to compare with the linear analysis of Levich (1962), they emphasized that choosing a single value of the growth rate is too simplistic to describe the evolution of the deformation. They conjectured that this was a consequence of the nonlinear influence of harmonics.

It seems to be generally thought that the normal-mode analysis cannot account for the non-exponential initial growth. No other methods have given a thorough understanding of such a transient and its relation to the initial conditions. Meanwhile, the qualitative and quantitative description of the transient phase has remained a challenge.

Reference	*Method*	*C*	*k*	*Initial conditions*	*Growth*
Taub (1976) figures 4–6	Nonlinear perturbation analysis (Yuen 1968)	0	0.30 0.37 0.60	Deformation	Slow
Berger (1988) figure 3	Initial-value linear analysis	0.23	0.10 ··· 0.90	Deformation	Slow
Ashgriz (1995) figure 4	Nonlinear three-dimensional computation	0.005† 10‡	0.20 0.90	Deformation	Slow†; normal‡
Saroka (2001) figure 4	Nonlinear three-dimensional computation (evaporation)	0.1	0.70	Deformation	Slow
Collantes (2003) figure 2	Initial-value linear analysis (Marangoni instability)	0.01 ··· 1.0	k_{max}	Deformation	Slow
Suryo (2006) figures 4, 12, 22	Nonlinear three-dimensional computation (compound jet)	0.010 0.032 1.0	0.20 ··· 0.80	Deformation	Slow
Chuech (2006) figure 13	Nonlinear one-dimensional computation	0	0.70	Deformation	Slow
Sellens (1992) figure 2	Nonlinear one-dimensional computation	0.004	0.71	Deformation†; mixed‡; impulse§	Slow†; normal‡; rapid§
Chaudhary (1980) figures 6–8	Nonlinear perturbation analysis	0	0.31 0.43 0.65	Impulse	Rapid
Bousfield (1987) figure 1	Nonlinear one-dimensional computation	4.7	0.50	Impulse	Rapid
Torpey (1989) figures 1, 2, 4, 6–14	Nonlinear spectral one-dimensional computation†; experiment‡	0.048	0.50 ··· 0.70	Impulse†; piezoelectric‡	Rapid†,‡
Xing (1996) figures 4–6	Experiment	0.24	0.64	Piezoelectric	Rapid

TABLE 1. References showing initial transients. Columns show: bibliographic reference (only first author) and figure numbers; method of acquisition for the data shown (theoretical or experimental); Ohnesorge number $C = \mu/(\rho\gamma R)^{1/2}$; non-dimensional wavenumber; initial conditions (if theoretical) or stimulation mechanism (if experimental); and qualitative growth of deformation during the initial transient relative to the subsequent pure exponential growth. †, ‡, §, correspondence within the same row.

2.3. *Experimental measurement of the growth rate*

What we shall call the *amplitude-evolution method* is the most direct method of measuring the growth rate from a conceptual point of view. It consists in perturbing the jet monoharmonically and measuring the amplitude of radial deformation of the

jet at each axial position within a selected interval. The logarithm of the amplitude is plotted against the axial position. The assumption of an exponential growth suggests fitting a straight line. Its slope gives the spatial growth rate directly; or, if multiplied by the emerging velocity, the temporal growth rate.

The above method is local, since it allows us to assign a growth rate to the portion of the jet chosen for the fitting. In this sense, it is opposite to the *breakup method*, based on the measurement of either the breakup time or the breakup length for different values of the initial amplitude (for a review, see Kalaaji *et al.* 2003; see also González & García 2008).

The amplitude-evolution method relies on the existence of an interval of purely exponential growth, as predicted by the classical Rayleigh linear analysis. Therefore, it is expected to suffer systematic errors if the data for the fitting have amplitudes that are too large, since the governing equations are nonlinear.

The first precise experiments implementing the amplitude-evolution method in order to measure the growth rate were intended to corroborate the dispersion relation of the jet. Donnelly & Glaberson (1966) verified the hypothesis of exponential growth within the accuracy of their experiment, even for unexpectedly large amplitudes. According to Yuen (1968), their success was due to having measured the amplitude through the semidifference between the swell and neck radii at each position: some nonlinear terms cancel out in his third-order perturbation analysis for inviscid jets. The measurements of Goedde & Yuen (1970) confirmed this.

Ronay (1978*b*) first took advantage of the measurement of the growth rate of a jet to obtain accurately the surface tension of a liquid. The measurement of the growth rate through the amplitude-evolution method serves to obtain the dynamic surface tension of liquid solutions or suspensions with fresh surfaces (Ronay 1978*a*). Being local, this method is suitable for tracing the evolution of the dynamic surface tension as a function of time (Bellizia *et al.* 2002; Battal *et al.* 2003; Alakoç *et al.* 2004; Weiss *et al.* 2004; Jatzkowski & Modigell 2005).

With the photographic technique used in these and other experiments (Rutland & Jameson 1970; Collicott, Zhang & Schneider 1994), it is difficult to measure small-amplitude perturbations accurately. The shadow technique (Taub 1976), although restricted to opaque liquids, allowed the accurate measuring of amplitudes in a range of several orders of magnitude. Wetsel (1980) applied it to measure growth rates. Evidence of non-exponential growth during the early evolution of the jet has been given with the shadow technique (Torpey 1989; Xing *et al.* 1996). As there is no theoretical estimate of the zone of the jet where exponential growth is expected, the experimenter has to select the fitting interval subjectively, which makes the method prone to systematic errors. Even though the precision of the amplitude measurement has clearly increased since the first experiments of Donnelly & Glaberson, nobody has validated the dispersion relation with the accuracy expected from current technical means. A quantitative estimate of the duration of the initial transient is crucial for accurately measuring the damping rate as a function of the wavenumber (González & García 2008).

3. Theoretical analysis and numerical methods

In the following analysis, all magnitudes are considered non-dimensional. The radius of the unperturbed cylindrical jet R is the scale for distance. The capillary time $(\rho R^3/\gamma)^{1/2}$ and the capillary velocity $[\gamma/(\rho R)]^{1/2}$ are chosen as the respective scales for time and velocity, where ρ stands for the density of the liquid and γ denotes

the surface tension. The first non-dimensional number that we consider is the dimensionless wavenumber $k = 2\pi R/\lambda$, where λ is the dimensional wavelength of the induced perturbation. Secondly, the Ohnesorge number gives the balance between the typical viscous stress and the surface tension,

$$C = \frac{\mu}{\sqrt{\rho\,\gamma\,R}}, \tag{3.1}$$

where μ is the dynamic viscosity. If the jet emanates from a nozzle with dimensional velocity v_0^*, the Weber number is the square of this velocity relative to the capillary velocity,

$$We = \frac{\rho\,R\,v_0^{*2}}{\gamma}. \tag{3.2}$$

Here, the Weber number is assumed to be large enough that the temporal analysis is valid. At the same time, it is also small enough that, combined with the huge difference in density, the surrounding gas has a negligible influence on the system. Thus, this number will not appear in our formulation. These restrictions apply to the solutions of the dispersion relation, but will be relaxed in our subsequent discussion.

3.1. *Eigenvalues and normal modes*

We shall not repeat the linearization of the Navier–Stokes equations and the deduction of the dispersion relation for arbitrary viscosity, worked out by Rayleigh (1892) and Chandrasekhar (1961). As will become clear below, it is mandatory to identify all roots of the dispersion relation and their corresponding normal modes if arbitrary initial conditions have to be taken into account.

Our study starts with the dispersion relation for the infinite axisymmetric jet (Rayleigh 1878),

$$c_{in}\,\hat{\alpha}^2 + c_{visc}\,\hat{\alpha} = c_{cap}, \tag{3.3}$$

where the coefficient functions

$$c_{in}(k) = \frac{I_0(k)}{k\,I_0'(k)}, \tag{3.4}$$

$$c_{visc}(k; k_v(k,\hat{\alpha})) = 4C\left[\frac{k\,I_0(k)}{I_0'(k)} - \frac{1}{2} + \frac{k^2}{k_v^2 - k^2}\left(\frac{k\,I_0(k)}{I_0'(k)} - \frac{k_v\,I_0(k_v)}{I_0'(k_v)}\right)\right], \tag{3.5}$$

and

$$c_{cap}(k) = 1 - k^2 \tag{3.6}$$

account for inertial, viscous and surface-tension contributions, respectively, and k_v is defined by

$$k_v^2 = k^2 + \frac{\hat{\alpha}}{C}. \tag{3.7}$$

Equation (3.3) recalls the dispersion relation for a damped harmonic oscillator driven by the surface tension. In fact, there are two solutions that exhibit the same qualitative behaviour, as found by Weber (1931) with his one-dimensional linear analysis for arbitrary viscosity. For inviscid liquids ($C = 0$), the coefficient c_{visc} is zero. It is the balance between inertia and surface tension that gives the only two roots of the dispersion relation. As viscosity is increased, these two roots $\hat{\alpha}_d$ and $\hat{\alpha}_s$ change, but the surface-tension term in (3.3) is always significant for them. When viscosity is paramount, it is the balance between viscous and surface-tension terms which gives the two roots mentioned, while the inertial terms become negligible. This is why we

call *capillary modes* to the eigenfunctions associated with those roots. Hereinafter, the *dominant mode*, the one with the greatest growth rate, will be distinguished with the subscript d; while the always decaying *subdominant mode* will be labelled with the subscript s.

However, there is a remarkable failure in this analogy with the harmonic oscillator: the viscous coefficient depends on $\hat{\alpha}$ itself. This gives other solutions, here reported as *hydrodynamic modes*, whose behaviour and significance must be clarified to have a rigorous understanding of the Rayleigh analysis.

As noticed by Grossmann & Müller (1984), there is a numerable infinite set of hydrodynamic modes besides the capillary ones, which will be denoted with the subscript h. Each of their corresponding eigenvalues is close to a pole of the viscous coefficient c_{visc} defined in (3.5). This nearness gives a simple approximation for the eigenvalues:

$$\hat{\alpha}_{hn} \simeq -C\left(x_n^2 + k^2\right), \tag{3.8}$$

where x_n are the zeros of the Bessel function of the first kind and first order. In particular, for the first hydrodynamic mode,

$$\hat{\alpha}_{h1} \simeq -C(14.68 + k^2). \tag{3.9}$$

This approximation is good for small Ohnesorge number and any value of k; and also for any value of C, provided k is small or of order unity. The proximity to poles explains why these roots have been reported so rarely, since the usual numerical methods hardly converge to them. They are difficult to find unless the dispersion relation (3.3) is multiplied by a factor that removes the nearest pole.

In order to interpret how the different modes evolve, not only do eigenvalues matter, but also their associated eigenfunctions. It is important to know the velocity field of each mode as well as its relation with the corresponding deformation of the surface. In the linear analysis, the time and axial dependence of the deformation and velocity for a given mode are

$$f(z,t) = \mathrm{Re}[\hat{f}\exp(\mathrm{i}kz + \hat{\alpha}t)] \tag{3.10}$$

and

$$\boldsymbol{v}(r,z,t) = \mathrm{Re}[\hat{\boldsymbol{v}}(r)\exp(\mathrm{i}kz + \hat{\alpha}t)], \tag{3.11}$$

where $\hat{f}$ is the complex amplitude of the deformation of the surface and $\hat{\boldsymbol{v}}(r)$ is the radial dependence of the velocity, also complex. For a given eigenvalue $\hat{\alpha}$, the linear analysis relates $\hat{\boldsymbol{v}}(r)$ with $\hat{f}$ through

$$\begin{aligned}\frac{\hat{\boldsymbol{v}}(r)}{\hat{f}} = &\left[(\hat{\alpha} + 2Ck^2)\,\frac{I_0'(kr)}{I_0'(k)} - 2Ck^2\,\frac{I_0'(k_v r)}{I_0'(k_v)}\right]\boldsymbol{e_r} \\ &+ \left[(\hat{\alpha} + 2Ck^2)\,\frac{\mathrm{i}\,I_0(kr)}{I_0'(k)} - 2Ck^2\,\frac{\mathrm{i}k_v\,I_0(k_v r)}{k\,I_0'(k_v)}\right]\boldsymbol{e}_z,\end{aligned} \tag{3.12}$$

where $\boldsymbol{e_r}$ and $\boldsymbol{e}_z$, respectively, stand for the radial and axial unit vectors.

A distinguishing feature of the hydrodynamic modes is that their velocity field exhibits recirculation. We will describe it in detail in § 4.1.2.

3.2. *Initial conditions*

The most important dependent variable in practice is the non-dimensional surface deformation $f(z,t)$. It is the only one that can be accurately measured in a jet up to now. For any possible small perturbation periodic in space, $f(z,t)$ can be expressed

as

$$f(z,t)=\mathrm{Re}\sum_{n=1}^{\infty}\exp(\mathrm{i}nkz)\left\{\hat{f}_{dn}\exp[\hat{\alpha}_d(nk)t]+\hat{f}_{sn}\exp[\hat{\alpha}_s(nk)t]+\sum_{l=1}^{\infty}\hat{f}_{hnl}\exp[\hat{\alpha}_{hl}(nk)t]\right\},\tag{3.13}$$

where $\hat{f}_{dn}$, $\hat{f}_{sn}$ and $\hat{f}_{hnl}$ are complex amplitudes. In the degenerate case of critical damping ($\hat{\alpha}_d=\hat{\alpha}_s=\hat{\alpha}$), it is given by

$$f(z,t)=\mathrm{Re}\sum_{n=1}^{\infty}\exp(\mathrm{i}nkz)\left\{-\hat{f}_{dn}\,\hat{\alpha}(nk)\,t\exp[\hat{\alpha}(nk)t]+\hat{f}_{sn}\exp[\hat{\alpha}(nk)t]+\sum_{l=1}^{\infty}\hat{f}_{hnl}\exp[\hat{\alpha}_{hl}(nk)t]\right\}.\tag{3.14}$$

Therefore, each Fourier mode of the surface deformation is associated with two capillary modes and a countable infinite set of hydrodynamic modes.

We shall neglect the contribution of the hydrodynamic modes in the following. We shall discuss why in § 5.

An initial surface deformation does not define uniquely the initial conditions. The velocity must also be considered. We shall do it through the *mean axial velocity* on a slice w, closely related to the surface deformation by the continuity equation integrated on a slice (García & Castellanos 1994). We emphasize that this equation is not a one-dimensional approximation: it is exact. For small perturbations, its linear counterpart is

$$f_t=-\tfrac{1}{2}w_z,\tag{3.15}$$

which will be referred to as the *kinematic condition* in the following.

Considering only the capillary modes and using (3.15), we obtain for the surface deformation and the mean axial velocity

$$f(z,t)=\mathrm{Re}\sum_{n=1}^{\infty}\exp(\mathrm{i}nkz)\{\hat{f}_{dn}\exp[\hat{\alpha}_d(nk)t]+\hat{f}_{sn}\exp[\hat{\alpha}_s(nk)t]\}\tag{3.16}$$

and

$$w(z,t)=\mathrm{Re}\sum_{n=1}^{\infty}\frac{2\mathrm{i}}{nk}\exp(\mathrm{i}nkz)\{\hat{f}_{dn}\hat{\alpha}_d(nk)\exp[\hat{\alpha}_d(nk)t]+\hat{f}_{sn}\hat{\alpha}_s(nk)\exp[\hat{\alpha}_s(nk)t]\}.\tag{3.17}$$

The initial conditions of the jet can be expressed as

$$f(z,0)=\mathrm{Re}\sum_{n=1}^{\infty}\hat{f}_{0n}\exp(\mathrm{i}nkz)\tag{3.18}$$

and

$$w(z,0)=\mathrm{Re}\sum_{n=1}^{\infty}\hat{w}_{0n}\exp(\mathrm{i}nkz),\tag{3.19}$$

where $\hat{f}_{0n}$ and $\hat{w}_{0n}$ are the complex initial amplitudes of the nth Fourier mode of the surface deformation and mean axial velocity. Thus, four real parameters per Fourier mode must be specified to fix the initial conditions uniquely.

Comparison of (3.18) and (3.19) with (3.16) and (3.17) evaluated at $t=0$ leads to

$$\hat{f}_{dn} = \frac{-1}{\hat{\alpha}_d(nk) - \hat{\alpha}_s(nk)} \left[\hat{\alpha}_s(nk)\, \hat{f}_{0n} + \tfrac{1}{2}\mathrm{i}nk\, \hat{w}_{0n}\right] \tag{3.20}$$

and

$$\hat{f}_{sn} = \frac{1}{\hat{\alpha}_d(nk) - \hat{\alpha}_s(nk)} \left[\hat{\alpha}_d(nk)\, \hat{f}_{0n} + \tfrac{1}{2}\mathrm{i}nk\, \hat{w}_{0n}\right], \tag{3.21}$$

which formally give the initial complex amplitudes of the two capillary modes for arbitrary initial conditions of the surface deformation and mean axial velocity. Reciprocally, any non-recirculating initial conditions can be described in terms of the two capillary modes. Not only can independent amplitudes of deformation and velocity of each Fourier mode be considered, as in the analysis of Berger (1988); here, phases are arbitrary as well, since constants are complex in general.

The corresponding expressions for the critical damping wavenumber can be readily obtained in a similar way. Nevertheless, we shall omit them for the sake of clarity, since they are not necessary for our discussion. Besides, they can be obtained by taking the appropriate limit.

If the dominant mode only were considered ($\hat{f}_s = 0$), as has generally been done before, the initial deformation would impose the initial velocity, or *vice versa*. Therefore, such an incomplete modal analysis could not deal with arbitrary initial conditions, whose initial deformation and velocity can be arbitrarily chosen. This is why some authors have blamed the Rayleigh analysis for being wrong or incomplete (Berger 1988; Ashgriz & Mashayek 1995).

In previous works, two types of initial condition have usually been imposed: either pure-deformation or pure-impulse. The expressions from the Rayleigh analysis, even more simple for these particular cases, will be useful for our discussion.

Let us start with *pure-deformation* initial conditions, i.e. $\hat{w}_{0n} = 0$ for all n. The amplitudes of the Rayleigh modes become

$$\hat{f}_{dn} = \frac{-\hat{\alpha}_s(nk)}{\hat{\alpha}_d(nk) - \hat{\alpha}_s(nk)}\, \hat{f}_{0n} \tag{3.22}$$

and

$$\hat{f}_{sn} = \frac{\hat{\alpha}_d(nk)}{\hat{\alpha}_d(nk) - \hat{\alpha}_s(nk)}\, \hat{f}_{0n}. \tag{3.23}$$

Therefore, given the complex amplitudes of the initial deformation, $\hat{f}_{0n}$, the linear evolution of the deformation is

$$f(z,t) = \mathrm{Re} \sum_{n=1}^{\infty} \exp(\mathrm{i}nkz) \frac{\hat{f}_{0n}}{\hat{\alpha}_d(nk) - \hat{\alpha}_s(nk)} \{-\hat{\alpha}_s(nk) \exp[\hat{\alpha}_d(nk)t] + \hat{\alpha}_d(nk) \exp[\hat{\alpha}_s(nk)t]\}. \tag{3.24}$$

To clarify the early behaviour of the jet, we shall restrict ourselves to a monoharmonic perturbation. Moreover, we shall consider the most relevant interval of wavenumbers, $0 < k < 1$; i.e. the interval where the perturbation grows aperiodically. As $\hat{\alpha}_d = \alpha_d$ and $\hat{\alpha}_s = \alpha_s$ are real, (3.24) becomes quite simple:

$$f(z,t) = \frac{\tilde{f}_0}{\alpha_d - \alpha_s} [-\alpha_s \exp(\alpha_d t) + \alpha_d \exp(\alpha_s t)] \cos(kz), \tag{3.25}$$

where $\tilde{f}_0$ is the initial real amplitude of deformation.

The early evolution of the jet is given by a combination of two exponentials: the dominant one, increasing with time; and the subdominant one, decreasing. The behaviour of this transient, as well as its duration before the exponential-growth phase, depend on the growth rates α_d and α_s. This is why it is so important to know their dependence on the wavenumber and viscosity.

In contrast, for *pure-impulse* initial conditions, i.e. $\hat{f}_{0n} = 0$ for all n, we have

$$\hat{f}_{dn} = -\hat{f}_{sn} = \frac{-\frac{1}{2}\mathrm{i}nk}{\hat{\alpha}_d(nk) - \hat{\alpha}_s(nk)}\,\hat{w}_{0n}, \tag{3.26}$$

while the evolution of the deformation is given by

$$f(z,t) = \mathrm{Re}\sum_{n=1}^{\infty} \exp(\mathrm{i}nkz)\frac{-\frac{1}{2}\mathrm{i}nk\,\hat{w}_{0n}}{\hat{\alpha}_d(nk) - \hat{\alpha}_s(nk)}\{\exp[\hat{\alpha}_d(nk)t] - \exp[\hat{\alpha}_s(nk)t]\}. \tag{3.27}$$

For a monoharmonic perturbation and $0 < k < 1$, (3.27) reduces to

$$f(z,t) = \frac{\frac{1}{2}k\,\tilde{w}_0}{\alpha_d - \alpha_s}[\exp(\alpha_d t) - \exp(\alpha_s t)]\,\sin(kz), \tag{3.28}$$

for an initially cylindrical jet with initial amplitude of the mean axial velocity perturbation $\tilde{w}_0$.

Equation (3.28) leads to a *transfer function* between the actual initial amplitude of the velocity perturbation and the equivalent initial amplitude of the dominant capillary mode:

$$\tilde{f}_{d0} = \frac{k/2}{\alpha_d - \alpha_s}\,\tilde{w}_0. \tag{3.29}$$

Bousfield & Denn (1987) deduced an analogous expression under the assumption of paramount viscosity and long wavelength. With our non-dimensionalization, it becomes

$$\tilde{f}_{d0} = 1 - \exp\left(\frac{-\tilde{w}_0}{6Ck}\right). \tag{3.30}$$

In the limit of small amplitude of perturbation and paramount viscosity, the latter expression reduces to the argument of the exponential changed in sign. In the long-wavelength one-dimensional model of Bousfield & Denn (1987), $\alpha_d - \alpha_s \to 3Ck^2$ as $C \gg 1$. Therefore, the limit of (3.30) for small amplitudes is a particular case of (3.29).

3.3. *Initial-transient duration and local measurement of the growth rate*

In the amplitude-evolution method of measurement of the growth rate, it is assumed that the amplitude of deformation exponentially grows downstream along a portion of the jet; or during an interval of time, if seen from the system of reference moving with the jet velocity. Provided this is the case, the growth rate can be obtained from a linear fitting of the logarithm of the disturbance amplitude versus either the position or the time. However, the assumption of exponential growth is not met during the transient, along which the subdominant capillary mode introduces a systematic error in the measurement of the growth rate of the dominant mode. To avoid the transient phase, the experimenter needs an accurate estimate of its duration.

The initial-transient duration depends, on the one hand, on how quickly the dominant mode grows and the subdominant mode decays. On the other hand, the transient does not end abruptly; we shall consider it either finished or not, depending on how strict we are in considering the growth as purely exponential. Therefore, the transient duration will be a function of a prescribed error level for the growth rate.

The *local* or *instantaneous growth rate* of an infinite jet can be measured from the evolution of the deformation of its surface through the function $\alpha(t) = \tilde{f}_t / \tilde{f}$ (a similar definition was proposed by Mansour & Lundgren 1990). Here, $\tilde{f}$ is the real amplitude of the deformation at a given instant. For exponential growth, $\alpha(t) = \alpha_d$. Thus, the relative departure from the theoretical value of the growth rate is

$$\delta_\alpha = \frac{\tilde{f}_t}{\alpha_d \, \tilde{f}} - 1. \tag{3.31}$$

Now we could fix an error level δ_α and solve (3.31) to find the transient duration. For a monoharmonic perturbation with wavenumber in the most relevant interval $0 < k < 1$, the procedure is simple. First, instead of writing the deformation in terms of complex initial amplitudes as in (3.16) and (3.20)–(3.21), we would do it in terms of the real amplitudes of the initial deformation and the mean axial velocity and the relative phase between them. Secondly, we would maximize such deformation with respect to the axial position to find the real amplitude for a given instant. Then we could calculate the instantaneous relative error δ_α, with the hope of subsequently solving it for the transient duration. Unfortunately, the result for δ_α is a rather cumbersome transcendental function of time. Therefore, we cannot give an explicit expression of the transient time for general initial conditions. Instead, we shall deduce simple formulae for the two most interesting initial conditions, i.e. pure-deformation and pure-impulse.

If we assume pure-impulse initial conditions, (3.28) yields

$$\delta_\alpha = \frac{(\alpha_d - \alpha_s)/\alpha_d}{\exp[(\alpha_d - \alpha_s)\, t] - 1}. \tag{3.32}$$

After a time long enough for δ_α to be small, the unit term in the denominator becomes negligible against the exponential. Therefore, δ_α is expected to decrease almost exponentially with respect to time.

Let us find the time that the transient lasts:

$$t_{trans} = \frac{1}{\alpha_d - \alpha_s} \ln\left[\frac{\alpha_d - \alpha_s}{\alpha_d \, \delta_\alpha} + 1\right]. \tag{3.33}$$

Here, δ_α must be interpreted as an error value: the maximum departure of the growth rate relative to its theoretical value in order to consider the growth as exponential. Of course, it has to be small; at least, smaller than the experimental errors, so that the initial transient does not introduce a systematic deviation in the statistical fitting. A convenient value could be $\delta_\alpha \simeq 1\%$.

Fixing a goal of relative error is useful in comparing the transient duration for different C and k. However, it is too strict a criterion when the aim is to corroborate experimentally the whole Rayleigh dispersion curve, in which α_d becomes very small as k either becomes small or tends to its cutoff value k_c. The accuracy in measurement is limited by the noisy perturbations that grow with the maximum growth rate α_{max}. Therefore, the most sensible experimental criterion is to fix an absolute error value $\Delta_\alpha = \delta_\alpha \, \alpha_d$ as a given fraction of α_{max}. In terms of Δ_α,

$$t_{trans} = \frac{1}{\alpha_d - \alpha_s} \ln\left[\frac{\alpha_d - \alpha_s}{\Delta_\alpha} + 1\right]. \tag{3.34}$$

An appropriate goal for the absolute error could be $\Delta_\alpha = 0.01 \, \alpha_{max}$.

The corresponding expressions of δ_α and t_{trans} for pure-deformation initial conditions can be useful for interpreting previous numerical results. These are readily found in

a similar manner to that for (3.32), (3.33) and (3.34):

$$\delta_\alpha = -\frac{1-\alpha_s/\alpha_d}{-(\alpha_s/\alpha_d)\exp[(\alpha_d-\alpha_s)\,t]+1}, \tag{3.35}$$

$$t_{trans} = \frac{1}{\alpha_d-\alpha_s}\ln\left[\frac{-\alpha_d}{\alpha_s}\left(\frac{1-\alpha_s/\alpha_d}{|\delta_\alpha|}-1\right)\right], \tag{3.36}$$

$$t_{trans} = \frac{1}{\alpha_d-\alpha_s}\ln\left[\frac{-\alpha_d}{\alpha_s}\left(\frac{\alpha_d-\alpha_s}{|\Delta_\alpha|}-1\right)\right]. \tag{3.37}$$

However, they are not so interesting from an experimental point of view.

3.4. *One-dimensional model and numerical method*

The numerical solution of the initial-value problem with a nonlinear one-dimensional model is a good test for our normal-mode analysis. The influence of nonlinearities can be made evident as well.

The one-dimensional model for our computations is a slightly improved version of the *averaged one-dimensional model* (García & Castellanos 1994). Its two coupled equations are in terms of the surface radius F and the mean axial velocity on a slice $\overline{W}$:

$$(F^2)_t + (F^2\overline{W})_z = 0, \tag{3.38}$$

$$\begin{aligned} F^2(\overline{W}_t + \overline{W}\,\overline{W}_z) - \left[\tfrac{1}{8}F^4\left(\overline{W}_{tz} - \tfrac{1}{2}\overline{W}_z^2 + \overline{W}\,\overline{W}_{zz}\right)\right]_z \\ = -F^2P_{cz} + 3C\left\{F^2\left[\left(1+\tfrac{1}{8}FF_{zz}-\tfrac{3}{8}F_z^2\right)^2 + \tfrac{1}{2}F_z^4\right]\overline{W}_z\right\}_z, \end{aligned} \tag{3.39}$$

where the subscripts t and z stand for partial derivatives with respect to time and axial position, respectively; and P_c is the capillary pressure jump across the surface,

$$P_c = \frac{1}{\sqrt{1+F_z^2}}\left(\frac{1}{F} - \frac{F_{zz}}{1+F_z^2}\right). \tag{3.40}$$

Appropriate boundary conditions must be added. For monoharmonic perturbations, the easiest choice is to impose zero velocity as well as zero spatial derivative of the deformation at both ends of a half-wavelength, as in Ashgriz & Mashayek (1995). Beside these symmetric boundary conditions, we have also implemented periodic boundary conditions for the whole wavelength. This allows more general initial conditions, but increases the computational effort.

The averaged model was originally deduced by García & Castellanos (1994) through a systematic expansion of the Navier–Stokes equations in the radial variable up to second order. The linear analysis showed that the most widely used *viscous slice model* (Eggers & Dupont 1994; García & Castellanos 1994), which can be considered a first-order model in that sense, is less accurate for small viscosity. The averaged model is equivalent to the well-known Cosserat model (Green 1976) for inviscid liquids. However, the Cosserat model is less accurate than both the viscous slice model and the averaged model for moderate or large viscosity.

The original version of the averaged model becomes numerically unstable near the breakup, a fact more evident for large C. It is due to slightly negative viscous dissipation in a small region of the forming drop. An exhaustive energetic analysis to find the dissipation function, similar to that of Eggers & Dupont (1994) for the viscous slice model, revealed that the dissipation function of the averaged model was not strictly positive definite. This was corrected through the addition of appropriate third-order terms in its viscous contribution. In this way, the numerical instability

disappears, while the results up to the instant of instability are indistinguishable. A brief description and some results were given by García & Castellanos (1999). The details are in García (1998).

The linear perturbation analysis (i.e. $F = 1 + f$ and $\overline{W} = w$ with $f \ll 1$ and $w \ll 1$) of the above equations leads to the following dispersion relation (García & Castellanos 1994):

$$\hat{\alpha}^2\left(1 + \tfrac{1}{8}k^2\right) + 3Ck^2\hat{\alpha} + \tfrac{1}{2}(k^4 - k^2) = 0. \tag{3.41}$$

The two roots of this quadratic equation accurately reproduce the corresponding ones of the three-dimensional dispersion relation. In the interval $0 < k < 1$, the relative error for the positive eigenvalue, i.e. the most significant one, is less than 0.2% for $C < 0.1$ and less than 0.6% for large values of C, the error rapidly decreasing as k decreases. For comparison, the inviscid slice model gives a maximum relative error of 6% in the same interval, while the corresponding error of the Cosserat model is greater than 3% for moderate or large viscosity.

In the dispersion relation (3.41), there are no other roots corresponding to hydrodynamic modes. This is common to all the mean-velocity one-dimensional models, whose simplified radial dependence for the velocity cannot account for recirculation.

The accuracy of one-dimensional models in the nonlinear regime is similar to that in the linear regime (García 1998; García & Castellanos 1999). It was tested by comparison against previous three-dimensional computations of jet breakups, both for small and paramount viscosity. The shape of the jet close to breakup is well described, even for wavenumbers near the cutoff limit; the exception is the slight overturn of the drop surface near pinching when the Ohnesorge number is very small (Wilkes, Phillips & Basaran 1999; Chen, Notz & Basaran 2002), which cannot be accounted for with the cylindrical parameterization of the free surface inherent to one-dimensional models.

The system of nonlinear partial differential equations formed by (3.38) and (3.39), together with the appropriate boundary and initial conditions, is solved numerically. First, we have discretized in space through a Galerkin finite-element method with cubic Hermite interpolation (Strang & Fix 1973). The resulting system of ordinary differential equations is solved through a second-order predictor–corrector method (Adams–Bashforth scheme for the predictor and trapezoid rule for the corrector) with variable time step. For the first four initializing steps only, a first-order predictor–corrector method (explicit and implicit Euler schemes) guarantees the smoothness of the initial conditions necessary to avoid subsequent numerical instability, which eliminates the need for artificial numerical dissipation in each temporal step (Gresho, Lee & Sani 1980; Zhang, Padgett & Basaran 1996). The system of nonlinear algebraic equations so obtained is solved through the Newton method. The computational cost concentrates on the inversion of the Jacobian matrix. As it is block diagonal, an adapted LU method does the work efficiently. Owing to the singularity of the solution near breakup, the spatial error tends to increase. In order to maintain a maximum spatial error through the computation, the spatial grid is refined when required. Typical per-step errors for the results of this paper are 10^{-6} for time and 10^{-4} for space. Between 1000 and 4000 finite elements were employed, depending on the wavenumber. The method stops when either a maximum number of finite elements is reached or the time step becomes smaller than a pre-established value.

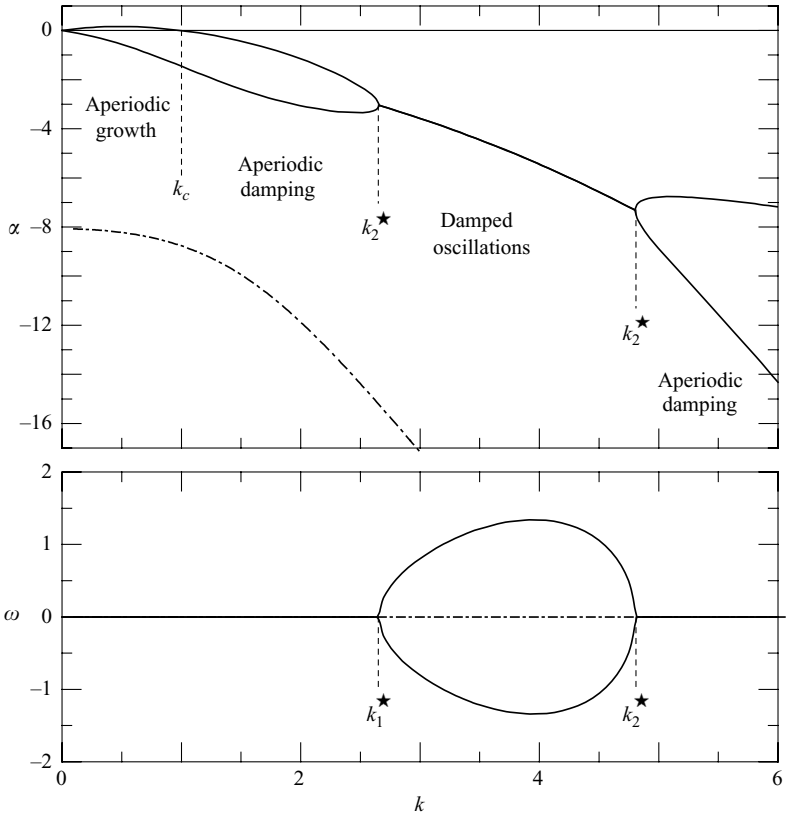

FIGURE 2. Growth rate α and oscillation frequency ω versus wavenumber k of the two capillary modes (——) and first hydrodynamic mode (– · –) for $C = 0.55$.

4. Results

4.1. *Eigenvalues and normal modes*

4.1.1. *Capillary modes*

Figure 2 depicts the growth rate and the oscillation frequency corresponding to the two capillary modes and the first hydrodynamic mode, obtained as roots of the dispersion relation (3.3) with $C = 0.55$. We have chosen this value of the Ohnesorge number to illustrate clearly the dynamics of each mode as a function of k. In the figure, $k_c = 1$ is the cutoff wavenumber, above which the infinitesimal perturbations are stable, while $k_1^\star$ and $k_2^\star$ are critical-damping wavenumbers. Labels identify the kind of evolution of the most significant mode in each interval of values of k. Figure 3 allows us to predict that kind of evolution for any values of C and k.

Figure 2 is representative of all possible mathematical behaviour of eigenvalues. According to the values of the wavenumber and the Ohnesorge number, the capillary modes behave in three possible ways, quantitatively bounded in figure 3.

(i) *Aperiodic growth* ($\alpha_d > 0,\ \alpha_s < 0,\ \omega_d = 0 = \omega_s$). For wavenumbers below the cutoff limit, the surface-tension term is destabilizing. There are an exponentially growing *dominant mode* and an exponentially decaying *subdominant mode*. There are no oscillations.

(ii) *Aperiodic damping* ($\alpha_d < 0, \alpha_s < \alpha_d, \omega_d = 0 = \omega_s$). Beyond the cutoff wavenumber, provided the viscous term is large enough with respect to the capillary term, both the

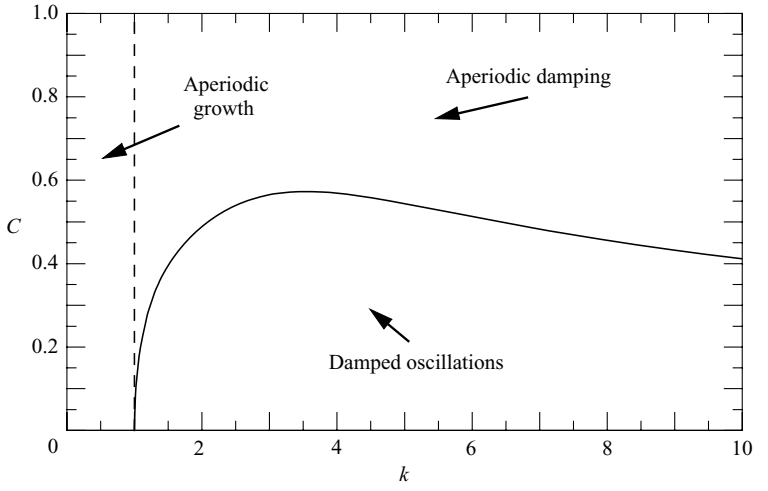

FIGURE 3. Plateau cutoff wavenumber (– – –), critical damping curve (——), and different behaviour of capillary modes, for any value of k and C of an axisymmetric infinite jet.

dominant and the subdominant modes are exponentially damped, without oscillations. This happens for large k, since the viscous shear is large for very short wavelength; but also for k in the vicinity of the cutoff limit, because the capillary term is small.

(iii) *Periodic oscillation* ($\alpha_d = 0 = \alpha_s$, $\omega_d = -\omega_s > 0$). For small enough Ohnesorge number ($C < 0.573$), there is an interval of wavenumbers beyond the cutoff limit where the two capillary eigenvalues are complex conjugate. Their associated modes are two damped waves that travel in opposite directions. Stationary waves are possible as an appropriate combination of these two modes. In this case, both modes are equally significant, so the names dominant and subdominant make no sense.

In the boundary line of *critical damping*, which separates the region of oscillations from the regions of aperiodic damping, the two capillary roots degenerate in only one ($\hat{\alpha}_d = \hat{\alpha}_s$). As in the harmonic oscillator, the solution is not the superposition of two different exponentials, but a linear combination of $\exp(\hat{\alpha}t)$ and $t\exp(\hat{\alpha}t)$.

Figure 4 shows the effect of increasing C on the growth rate and the oscillation frequency of the capillary modes. In particular, we can see how the dominant mode is more significant than the subdominant mode, through the difference between their respective growth rates.

It is well known that an increase in viscosity makes the growth rate of the dominant mode decrease. This also happens with the subdominant mode (figure 4). Notice that, for small or moderate viscosity, α_d is significantly larger than α_s in the vicinity of $k = k_{max}$, which means that the subdominant mode has a secondary role. However, this is not so true for small k or near the critical-damping wavenumber, where the difference in growth of both capillary modes is smaller.

For our discussion of the initial conditions, it is important to know the form of the velocity field of the capillary eigenfunctions. This is depicted, for $C = 0.55$, in figure 5 ($k = 0.5$, aperiodic growth) and figure 6 ($k = 2.5$, aperiodic damping).

4.1.2. *Hydrodynamic modes*

The normal-mode analysis is valid for any small periodic perturbation that we could consider. This includes initial conditions consisting in a cylinder with a recirculating velocity field; with viscosity, such perturbations are expected to be damped. A glance

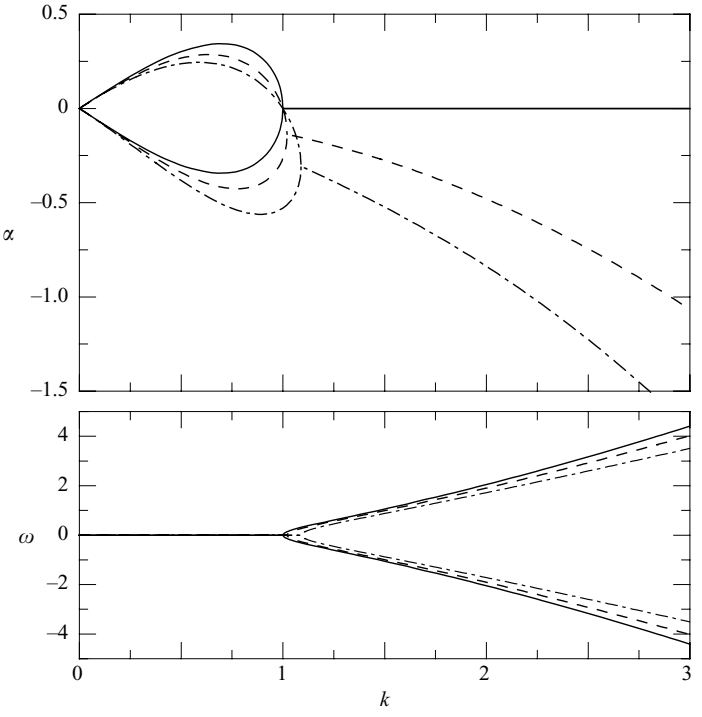

FIGURE 4. Growth rate α and oscillation frequency ω versus wavenumber k; for $C = 0$ (——), $C = 0.1$ (– – –) and $C = 0.2$ (– · –).

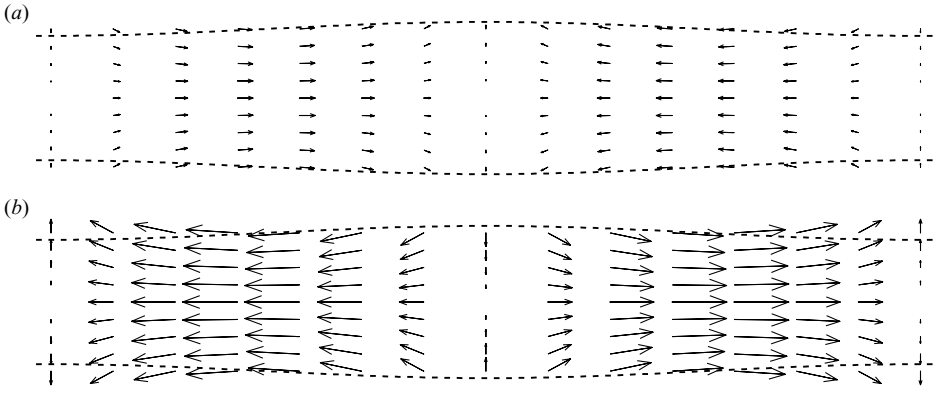

FIGURE 5. Velocity field of the two capillary modes, (*a*) dominant (*b*) subdominant, in the zone of aperiodic growth ($C = 0.55$, $k = 0.5$) for the same surface deformation (- - -).

at figures 5 and 6 shows that a superposition of capillary modes cannot describe initial conditions with a recirculating velocity field. Since the linear modal analysis is complete for small-amplitude perturbations, there must be other modes to account for recirculation: the hydrodynamic modes.

As an example, the first hydrodynamic root of the dispersion relation with $C = 0.55$ is shown in figure 2, and its velocity field for $k = 0.5$ can be seen in figure 7. The velocity-field pattern of subsequent hydrodynamic modes is easy to imagine: the nth

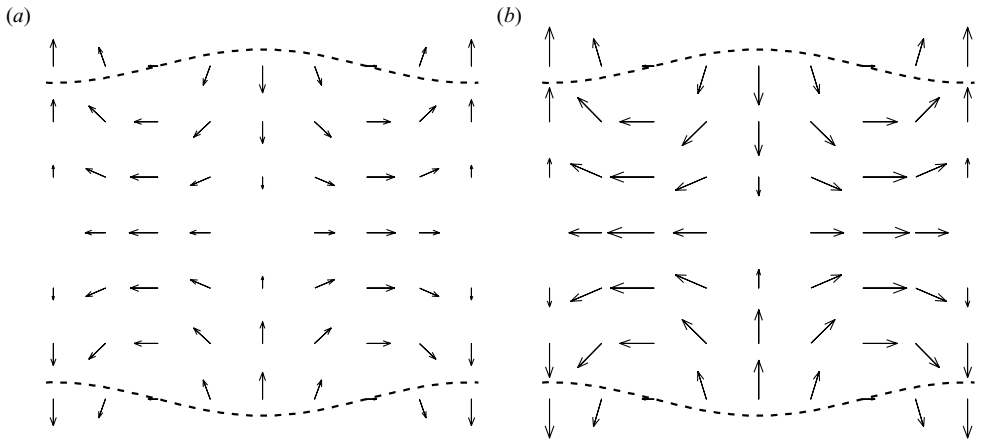

FIGURE 6. Velocity field of the two capillary modes, (*a*) dominant (*b*) subdominant, in the zone of aperiodic damping ($C = 0.55$, $k = 2.5$) for the same surface deformation (- - -).

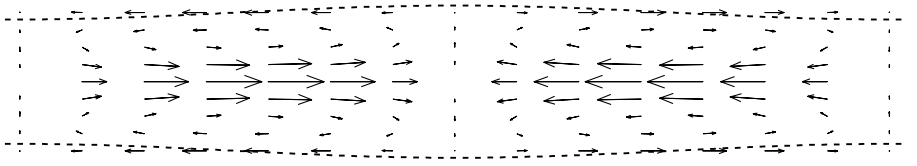

FIGURE 7. Velocity field of the first hydrodynamic mode for $C = 0.55$ and $k = 0.5$. The surface deformation is the same as for figure 5, but the velocity field has been scaled by a factor 1/1000.

mode has n recirculating rolls distributed from the symmetry axis to the surface of the jet, i.e. the sign of the axial velocity changes n times in the radial direction.

The hydrodynamic modes are always aperiodically damped, for their eigenvalues are always real and negative. For these modes, the leading term in the dispersion relation is the viscous dissipation term, while the capillary term has a secondary role. As depicted in figure 7, the amplitudes of the surface deformation and mean axial velocity are usually negligible in these modes when compared to the amplitude of the velocity field.

In order to compare the relative significance of the decaying modes, in figure 8 we represent the growth rate of the capillary modes and the first two hydrodynamic axisymmetric modes against the wavenumber for $C = 0.005$.

The inverse of the growth rate of the first hydrodynamic mode gives us an estimate of the damping time of a recirculating perturbation. In practice, the approximation (3.9) is enough to this purpose. We see that it is very damped, even for small C. For $C > 0.023$, its growth rate is even more negative than α_s. For smaller Ohnesorge numbers, one or more hydrodynamic eigenvalues seem to cross the subdominant one, as shown in figure 8. However, conversely to the critical damping points, the curves do not actually cross: there is no degeneration of modes.

4.2. *Initial transients*

Figure 9 compares the semi-analytical results of Berger (1988, from his figure 3) with the prediction of the modal analysis of Rayleigh. The temporal evolution of the deformation amplitude relative to its initial value is plotted. In Berger, all

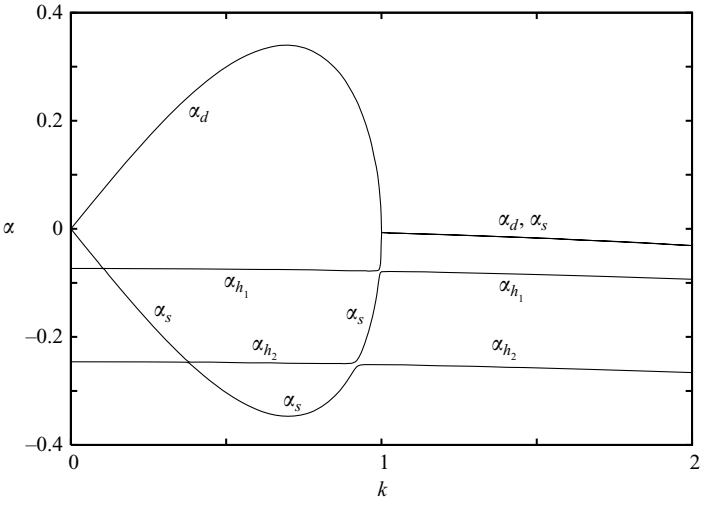

FIGURE 8. Growth rates of the capillary dominant, capillary subdominant, and first two hydrodynamic modes for $C = 0.005$.

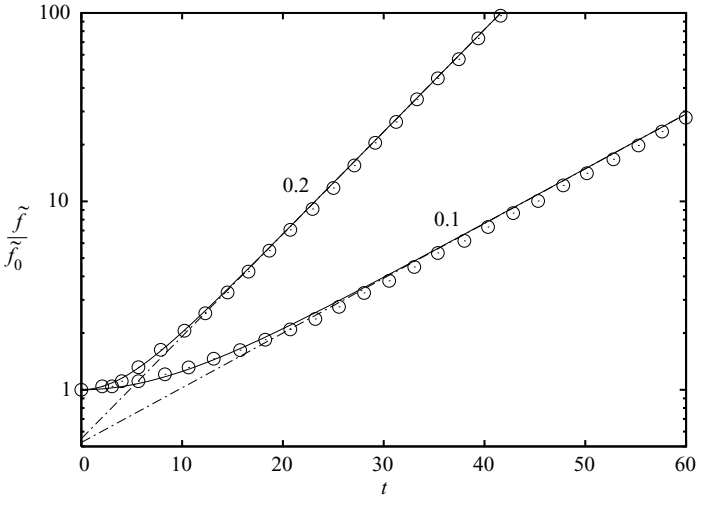

FIGURE 9. Evolution of the amplitude of deformation relative to its initial value with the same initial conditions as in Berger (1988): $\tilde{w}_0 = 2.25 \times 10^{-5}\, \tilde{f}_0$, $C = 0.2325$; and $k = 0.1$ and 0.2. Results from the linear analysis of Berger (1988) (⊙), the single dominant mode (– · –), and our full normal-mode analysis (——).

magnitudes are dimensional, with units from the c.g.s. measurement system. He gives the following values for the parameters: $R = 2.54 \times 10^{-3}$ cm, $\gamma = 78.2$ dyn cm^{-1}, $\rho = 1$ g cm^{-3}, and $\mu/\rho = 0.1$ cm^2 s^{-1}. His initial conditions are defined by $\tilde{f}_0^* = 1$ cm and $\dot{\tilde{f}}_0^* = 1.5$ cm s^{-1}, where the asterisk identifies those amplitudes as dimensional, and the overdot denotes derivative with respect to time. With our non-dimensionalization, we obtain $C = 0.2325$ and initial amplitudes of the deformation and mean axial velocity $\tilde{f}_0 = 394$ and $\tilde{w}_0 = 8.86 \times 10^{-3}$, respectively.

Together with some of the results of Berger, we have plotted the predictions corresponding to the Rayleigh analysis with only the dominant mode and with the

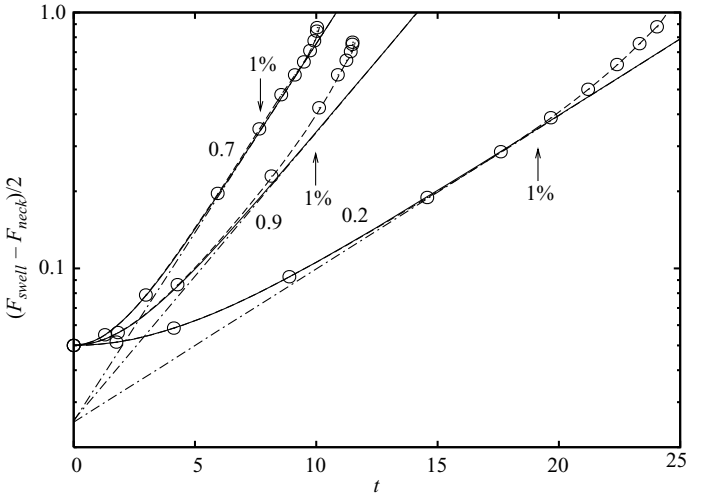

FIGURE 10. Evolution of the semidifference between swell and neck radii for pure-deformation initial conditions ($\tilde{f}_0 = 0.05$, $\tilde{w}_0 = 0$), $C = 0.005$, and $k = 0.2$, 0.7 and 0.9, as given by the three-dimensional numerical simulation of Ashgriz & Mashayek (1995) ($\odot$), our one-dimensional numerical simulation (– – –), the single dominant mode (– · –), and our full normal-mode analysis (——). The vertical arrows mark the theoretical end of the transient duration for $\delta_\alpha = 1\,\%$, according to (3.36).

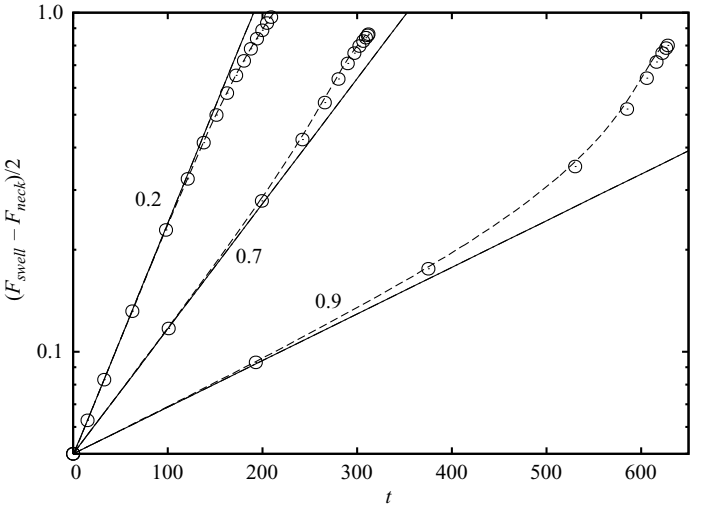

FIGURE 11. Evolution of the semidifference between swell and neck radii for pure-deformation initial conditions ($\tilde{f}_0 = 0.05$, $\tilde{w}_0 = 0$), $C = 10$, and $k = 0.2$, 0.7 and 0.9, as given by the three-dimensional numerical simulation of Ashgriz & Mashayek (1995) ($\odot$), our one-dimensional numerical simulation (– – –), and both the single dominant mode and our full normal-mode analysis (——, coincident).

two capillary modes. The two sets of data represented correspond to small values of the wavenumber, for which Berger noticed that the initial transient was more evident.

We have represented the temporal evolution of the surface-deformation amplitude of a jet subject to pure-deformation initial conditions in figures 10 (very small viscosity) and 11 (paramount viscosity), with the same conditions as in figure 4 of Ashgriz &

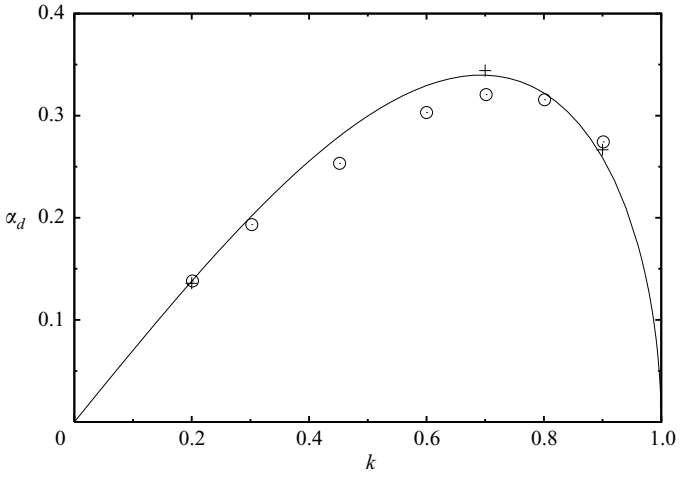

FIGURE 12. Growth rate α of the most significant mode versus non-dimensional wavenumber k, for $C = 0.005$, as given by the Rayleigh analysis (solid line), the single-mode fitting of Ashgriz & Mashayek (1995) ($\odot$), and a two-mode fitting of the small-amplitude data shown in figure 10 (+).

Mashayek (1995). Instead of computing such amplitude as the difference of either the swell or the neck radius with respect to the unperturbed radius, it is computed as the semidifference between the swell radius and the neck radius. This seems to partially counteract the nonlinear effect of growing harmonics (Yuen 1968; Goedde & Yuen 1970). In addition to the data from the numerical three-dimensional computations of Ashgriz & Mashayek, we have plotted the predictions from the monomodal analysis (with only the dominant mode) and our full modal analysis (with both the dominant and subdominant capillary modes). The logarithmic scale in the ordinates means that a straight line would correspond to a purely exponential growth, as predicted by the monomodal Rayleigh analysis.

Figures 10 and 11 illustrate, first, the slow-growth transient associated with the pure-deformation initial conditions when viscosity is small; and the absence of transient when viscosity is paramount. Secondly, the comparison with the monomodal analysis prediction gives us an idea of the extent of the three zones of evolution: the linear transient, the exponential growth and the nonlinear growth towards the breakup. Thirdly, the comparison with the three-dimensional and one-dimensional nonlinear numerical simulations contrasts the validity of the full modal analysis. Finally, the comparison between one-dimensional and three-dimensional numerical simulations gives an idea of the error associated with the one-dimensional model.

For numerical test purposes, Ashgriz & Mashayek (1995) tried to reproduce the most significant solution to the three-dimensional dispersion relation by fitting an exponential (dominant capillary mode) to their numerical data of deformation amplitude. In figure 12, we show their results for $C = 0.005$, together with the corresponding theoretical curve. In order to take into account the transient, we have applied a second fitting with two exponentials to the original data appearing in figure 10. We have considered data points with amplitudes that are not too large (less than 0.2) to avoid nonlinear effects. For $k = 0.9$, owing to the small number of data points, we have imposed equal amplitudes for both modes, as expected for such

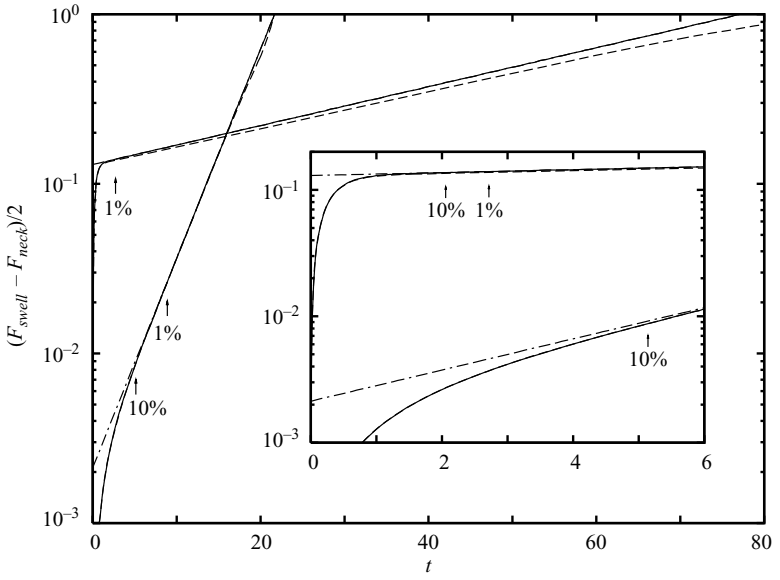

FIGURE 13. Evolution of the amplitude of the first Fourier mode of the deformation, measured through the semidifference between swell and neck radii; for pure-impulse monoharmonic initial conditions with $k = 0.050$; with $C = 0.048$ and $\tilde{w}_0 = 5.1 \times 10^{-3}$ (steepest growing curve), as in Torpey (1989); and $C = 4.7$ and $\tilde{w}_0 = 1.81$, as in Bousfield & Denn (1987). Monomodal analysis (–·–), full modal analysis with pure-impulse initial conditions (——), and nonlinear one-dimensional simulation (– – –). The vertical arrows mark the theoretical end of the transient duration for the labelled relative error δ_α, according to (3.33). The inset gives an enlargement of the transients.

a small Ohnesorge number, so as to have a number of data points at least equal to the number of fitting parameters.

Figure 13 depicts the influence of viscosity on the rapid-growth initial transient expected for pure-impulse initial conditions. The two cases presented have $k = 0.50$. The parameters of the family of curves with $C = 0.048$ (steepest) and small initial amplitude correspond to a numerical simulation of Torpey (1989). The curves with $C = 4.7$ (flattest) and relatively large initial amplitude simulate those found numerically in the work of Bousfield & Denn (1987). In both cases, we have plotted the evolution of the deformation amplitude in logarithmic scale, computed in three ways: First, the Rayleigh monomodal linear analysis (dot–dashed line), which gives the classical straight line corresponding to the purely exponential growth; secondly, our two-mode linear analysis (solid line); and finally, the numerical simulation of the nonlinear initial-value problem with the aid of the averaged one-dimensional model (dashed line). The latter is hard to see at the early times because it matches the solid line from the two-mode analysis. It will serve us to discuss the validity of the Rayleigh normal-mode analysis, as well as to show the nonlinear effects for non-small amplitudes.

As an example of comparison between experiments and theory, we have chosen the experimental data of Xing *et al.* (1996) with small initial amplitude, measured through the shadow method applied to an ink jet. Figure 14 shows the amplitude of the fundamental Fourier mode of the deformation versus the axial position x. As Kalaaji *et al.* (2003) showed afterwards, the growth rate of the deformation amplitude does not agree with its theoretical value because the dynamic surface tension differs

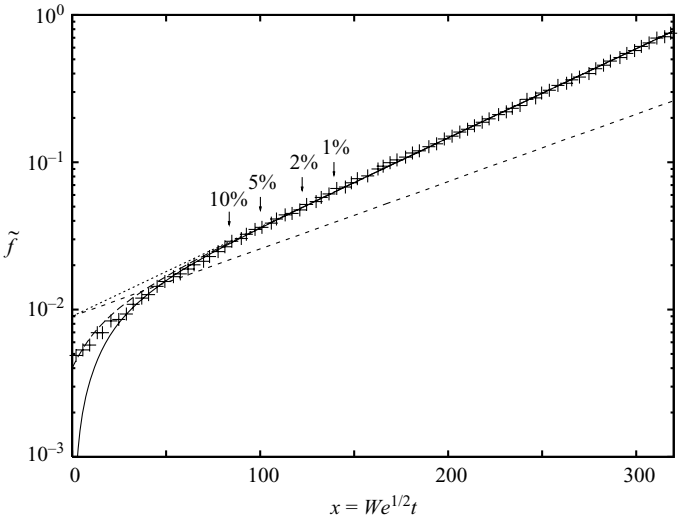

FIGURE 14. Amplitude of the first Fourier mode of the deformation versus non-dimensional axial position, for the experimental conditions of Xing *et al.* (1996) ($C = 0.196$ and $k = 0.636$, see text for details). Experimental data (+); monomodal analysis with fitted dynamic surface tension ($\cdots$); monomodal analysis with the original static surface tension (- - -); full modal analysis with pure-impulse initial conditions (——); and full modal analysis with tentative mixed initial conditions (– – –), equivalent to pure-impulse initial conditions at $x = -13$. The vertical arrows mark the theoretical end of the transient duration for the labelled relative error of the growth rate.

from the static surface tension measured in the experiment. In order to estimate the non-dimensional numbers for our analytical prediction, we have obtained a value of the dynamic surface tension from a fitting of the original data in the exponential-growth zone. The corresponding dotted line in the figure is also the prediction of the monomodal analysis, and its ordinate at the origin gives a fitted value of the initial amplitude of the dominant mode ($\tilde{f}_{d0} = 0.0090$). This gives $C = 0.196$. Just given for reference, the short-dashed line is the monomodal prediction corresponding to the original values of the non-dimensional numbers.

The solid line in figure 14 is computed through our full normal-mode analysis for pure-impulse initial conditions, given by (3.28) with $\tilde{w}_0 = 0.0202$, where the initial amplitude is estimated from the fitted value of $\tilde{f}_{d0}$ along the interval with purely exponential growth. The vertical arrows mark the end of the transient duration for different labelled relative errors of the growth rate, as given by (3.33). Finally, in order to discuss the non-zero deformation amplitudes measured at $x = 0$, we have plotted the full modal prediction from tentative mixed initial conditions ((3.18) for a monoharmonic perturbation with $\hat{f}_0 = 4.0 \times 10^{-3}$ and $\hat{w}_0 = 0.0143\,\mathrm{i}$ in (3.20) and (3.21)), equivalent to pure-impulse initial conditions at $x = -13$; or, in dimensional units, some 260 μm upstream of the origin of abscissae.

In figure 15, we represent the transient duration for pure-impulse initial conditions against the wavenumber, with fixed relative error of the growth rate $\delta_\alpha = 0.01$. Each curve corresponds to a different Ohnesorge number.

In figure 16, we represent the same transient duration, but with fixed absolute error of the growth rate $\Delta_\alpha = 0.01\,\alpha_{max}(C)$. Again, the different curves illustrate the effect of changing the Ohnesorge number.

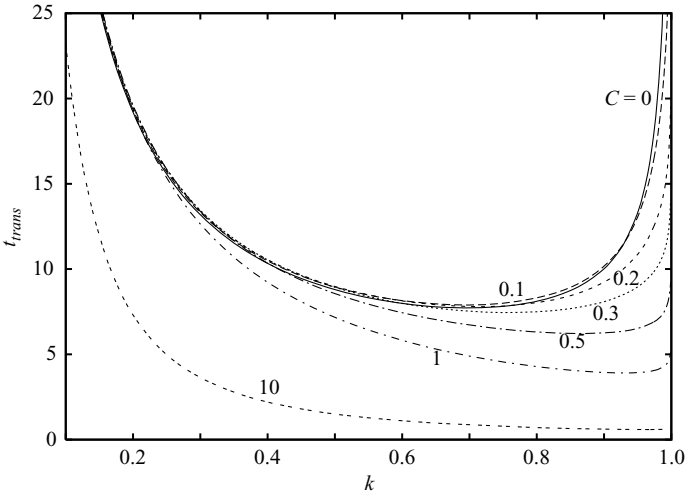

FIGURE 15. Non-dimensional transient time versus non-dimensional wavenumber, according to the three-dimensional linear modal analysis, for fixed relative error of the instantaneous growth rate, $\delta_\alpha = 0.01$, and different Ohnesorge numbers.

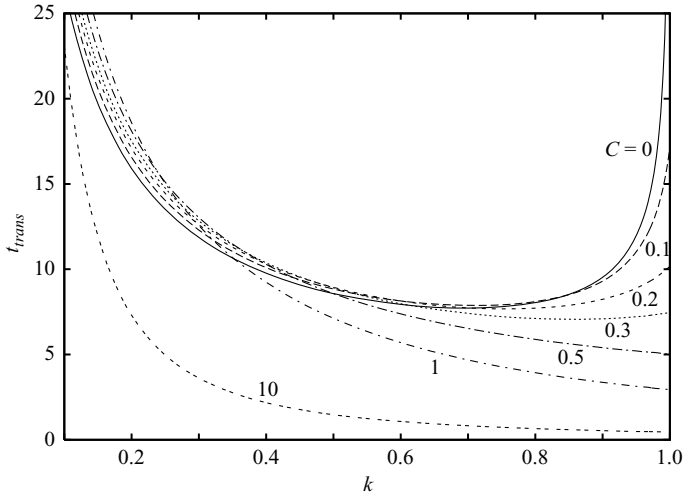

FIGURE 16. Non-dimensional transient time versus non-dimensional wavenumber, according to the three-dimensional linear modal analysis, for different Ohnesorge numbers. For each C, the absolute error of the instantaneous growth rate is set to $\Delta_\alpha = 0.01\,\alpha_{max}(C)$.

5. Discussion

5.1. *Eigenvalues and normal modes*

After the previous detailed description of the normal modes, we can answer the question of how many modes are necessary to account for some given initial conditions. It is clear that the dominant mode by itself cannot account for initial conditions of pure deformation or pure impulse, since it always has a velocity field associated with its surface deformation. An initial superposition of the two capillary modes is generally necessary.

Notice that describing the initial conditions through the deformation and the mean axial velocity, instead of the whole velocity field itself, makes the analysis simpler. This does not mean that either the radial velocity is neglected or the velocity field is approximated by its axial component. The evolution of the velocity field can be computed through the combination of the capillary modes (a linear combination of two eigenfunctions such as those plotted in figures 5 and 6). The amplitude of the mean axial velocity is representative of the amplitude of the velocity field, as long as there is no appreciable recirculation. The only loss of generality when ignoring the initial amplitudes of the hydrodynamic modes is the inability to represent a recirculating velocity field. If the hydrodynamic modes were considered, any possible initial state of the jet could be accounted for, including those with recirculating velocity, as we have seen at the beginning of our analysis. Instead of four real constants, more would be necessary to describe arbitrary initial conditions.

However, there are good reasons to eliminate the hydrodynamic axisymmetric modes when relating the initial conditions to the normal-mode analysis. First, the initial amplitudes of the hydrodynamic modes are usually expected to be small, since stimulating devices are not specifically designed for inducing recirculation in the nozzle. Even if they were present, their contribution to the surface deformation would be small. Finally, since they are damped, their effect on the subsequent dynamics is expected to be negligible. Since velocity perturbations are not easy to measure in jets, it is not surprising that such recirculating modes have not been reported experimentally.

Only if some external agent were to favour recirculation, as happens when shear stress on the liquid surface is significant, could the corresponding hydrodynamic modes be more relevant. A clear example of non-axisymmetric recirculation induced by interfacial shear stress is found in the numerical simulations of Pan & Suga (2006). A complete normal-mode analysis considering the growth of hydrodynamic non-axisymmetric modes could lead to a better understanding of the sinuous wave instability of jets with high velocity with respect to the surrounding gas.

5.2. *Initial transients*

The expressions for the evolution of both the deformation and the mean axial velocity in terms of the given initial conditions depend on the growth rates of the two capillary modes. Therefore, the initial transient will be explained through our detailed knowledge of the solutions of the dispersion relation. We shall discuss separately the two types of initial conditions most widely found in the literature: pure-deformation and pure-impulse.

Pure-deformation initial conditions are not realistic for liquid jets. They can be imposed on other related free-boundary fluid systems either by deforming them by contact (see Apfel *et al.* 1997, for an example of an initially deformed drop) or releasing them from the previous action of an electric field, as in Ramos, García & Valverde (1999) for a liquid bridge or in Basaran & Depaoli (1994) for a liquid drop; but these initial conditions are much more difficult to apply to a liquid jet since it moves so rapidly. Nevertheless, pure-deformation initial conditions are usual in theoretical and numerical work. This gives us results to interpret and compare with.

For inviscid liquid jets, $-\alpha_s$ is equal to α_d. Thus, the temporal dependence for the deformation after an initial pure deformation is a hyperbolic cosine; this is the same as considered by Rayleigh (1878) and other authors for these kinds of initial conditions when $C = 0$. Something similar can be said, provided viscous effects are small: both the dominant and subdominant modes contribute with the same sign and similar

initial amplitudes to the initial deformation. The transient will be slow as compared to the growth of the dominant mode, since the velocity is small at the beginning (see figures 9 and 10). As time passes, the subdominant mode decays, while the dominant one becomes more relevant: the exponential-growth phase approaches. This explains the clear correlation in table 1 between pure-deformation initial conditions and slow-growth transient for small viscosity in previous analytical and numerical work (Taub 1976; Berger 1988; Sellens 1992; Ashgriz & Mashayek 1995; Saroka *et al.* 2001; Collantes *et al.* 2003; Chuech & Yan 2006; Suryo *et al.* 2006).

For moderate or large viscosity, $|\alpha_s|$ clearly becomes greater than α_d (see figures 2 and 4). Therefore, the subdominant mode has a smaller amplitude right from the beginning: the transient is either less evident for moderate viscous effects (Berger 1988, with $C = 0.23$ and $k > 0.4$), or even unnoticed for large viscosity (Ashgriz & Mashayek 1995, with $C = 10$). This explains the numerical observation of Ashgriz & Mashayek (1995): there is no apparent transient when viscosity is paramount (see figure 11). The mean axial velocity sharply increases from its null initial value to the value corresponding to the dominant mode; but there is no effect of such a brief transient on the surface deformation, as the amplitude of the subdominant mode does not significantly contribute to the amplitude of the deformation from the beginning.

The pure-impulse initial conditions are far more realistic, for these describe the most common kind of experimental perturbations: the piezoelectric stimulation. In this case, the initial null deformation imposes that the deformation amplitudes of the two capillary modes must initially have opposite signs and equal modules, independently of viscosity. The velocity is initially greater than the one in the exponential-growth phase, which induces a rapid-growth transient as compared to the growth of the dominant mode (see figure 13). This agrees with the correlation between pure-impulse initial conditions and the rapid-growth transient observed in previous results (see table 1), either theoretical (Chaudhary & Redekopp 1980, with $C = 0$; Bousfield & Denn 1987, with $C = 4.7$; Torpey 1989, with $C = 0.034$; and Sellens 1992, with $C = 0.004$) or experimental (Torpey 1989, with $C = 0.034$; Xing *et al.* 1996, with $C = 0.24$). As C increases, the transient does not disappear; it becomes more and more brief and abrupt (see figure 13), while the velocity is greatly and quickly reduced from its initial amplitude by viscous shear. As the breakup time increases with C, the transient is less relevant for viscous enough liquid jets.

The normal-mode analysis allows more general initial conditions. The two cases discussed above are the extreme choices. A mixed case is the pure dominant mode, which initially has both a deformation and an impulse. With these initial conditions, the deformation grows exponentially from the beginning, so there is no transient at all. Some numerical trials with mixed initial conditions like these confirm this absence of a transient (Sellens 1992).

It might be thought that the only interesting initial conditions are those with pure impulse. However, the measurement of amplitude does not usually start exactly at the nozzle exit, but at some point slightly downwards. In such a case, mixed initial conditions are to be expected, since the jet has had time to deform. Moreover, there is evidence that other kinds of stimulation, such as electrohydrodynamic stimulation (García *et al.* 2000), may induce mixed initial conditions, which would involve out-of-phase perturbations of deformation and velocity. Formally, the Rayleigh normal-mode analysis can deal with any sort of initial conditions.

Figure 9 clearly depicts a slow-growth transient, typical for pure-deformation initial conditions when viscosity is small. In fact, this is the case of the initial conditions proposed by Berger (1988), since the initial impulse is insignificant against the

disproportional initial deformation. The transient lasts longer for longer wavelength, as predicted by (3.36) or (3.37).

Berger claimed that the initial amplitude is 'immaterial', a misunderstanding derived from the wrong estimate of the rupture time proposed by Levich (1962). He chose his initial conditions empirically to better fit his numerical breakup times to the experiments cited in his work. It is now clear that such initial conditions are arbitrary, since there was neither theoretical nor experimental evidence of initial deformation without significant velocity perturbation; and physically impossible, since the initial deformation cannot initially have an amplitude greater than the radius of the exit orifice. The large deviations from the experiments for both small and large Ohnesorge numbers, in spite of fitting the initial conditions, are a consequence of the spurious comparison.

Nevertheless, the analysis of Berger is formally correct. The good agreement between our full normal-mode analysis and Berger's semianalytical predictions in figure 9 definitely contradicts his main claim: the normal-mode analysis does account for the initial transient provided the two capillary modes are considered.

Figure 10 shows that the full normal-mode analysis accurately predicts the slow-growth initial transient that a slightly viscous liquid jet exhibits when subject to an initial static deformation. In contrast, the traditional one-mode analysis fails in the early stages of the evolution.

When viscous shear is paramount (figure 11), there is no noticeable transient: both the one-mode and the two-mode analysis agree with each other and with the nonlinear three-dimensional and one-dimensional simulations of the early evolution of the jet. Therefore, it is not true that initially there are many harmonics, and viscous shear damps them out quickly, as previously thought (Berger 1988; Ashgriz & Mashayek 1995). More simply, the monoharmonic pure-deformation initial conditions stimulate almost exclusively the dominant mode when viscosity is paramount. Only a very brief transient for the velocity would be noticeable if the latter could be measured.

The excellent agreement between one-dimensional and three-dimensional nonlinear numerical simulations in figures 10 and 11 is quantitatively similar to the agreement between their respective linear-analysis predictions (García & Castellanos 1994), which means that the error is less than usual in any experiment. This enables our one-dimensional nonlinear simulation to distinguish when nonlinear terms begin to be significant in the evolution of the deformation amplitude. Concerning the linear normal-mode analysis, the more comfortable one-dimensional estimate of the growth rates is, in practice, more than enough to safely predict the early evolution of the deformation and estimate the transient duration.

Figure 10 shows how difficult it is to measure the growth rate of the dominant mode when the initial amplitude is too large, not only in experiments, but even in numerical simulations. In principle, it could be thought that such a small initial deformation as 0.05 times the unperturbed radius would leave us a short time, but enough to fit an exponential growth. However, including data from the initial transient in our fitting would introduce a systematic deviation in the growth rate. On the other hand, if we start the fitting after the transient, the nonlinear terms will be significant enough to yield another systematic deviation. In other words, if the initial amplitude is not small enough, there will not exist a purely exponential growth phase because the initial transient phase overlaps the nonlinear growth phase. Under these conditions, any attempt to fit a growth rate is prone to systematic errors. This is the origin of the evident systematic deviation of the numerically fitted growth rates from their theoretical value found by Ashgriz & Mashayek (1995) for small viscosity (figure 12).

In contrast, for viscous enough liquids, the slow-growth transient is much less significant, so we can start the fitting of the growth rate almost from the beginning (see figure 11). As there is a long enough exponential-growth phase before the nonlinear phase, the growth rate can be fitted without systematic errors. This explains why the growth rate obtained by Ashgriz & Mashayek (1995) agreed better with its theoretical value for large viscosity.

We have implemented a new way of fitting the growth rate that allows us to make use of data from both the transient phase and the exponential-growth phase. Instead of fitting a single growing exponential to the small-amplitude data of figure 10, we have fitted a linear combination of two exponentials, one increasing (dominant mode) and the other decreasing (subdominant mode). The improvement is clear in figure 12.

In numerical simulations such as the one discussed above, a smaller initial amplitude would be enough to enlarge the purely exponential phase, thus making the correct growth rate easier to obtain. This has been successfully done by Suryo *et al.* (2006) for compound jets. In experiments, however, it is not so easy, as we shall discuss later.

The two rapid-growth transients depicted in figure 13, with equal wavenumbers but very different Ohnesorge numbers, illustrate the influence of viscosity for pure-impulse initial conditions. Although the typical straight line from the one-mode Rayleigh analysis matches the prediction from the two-mode analysis after some time, it cannot account for the null initial amplitude of the deformation; the deviation is clear during the transient. The transient is rapid in the sense that the instantaneous growth rate is clearly greater than the value of the dominant mode. Therefore, measuring the growth rate too close to the nozzle would lead to overestimating it. The arrows that mark the end of the transient for the labelled relative error in the growth rate give a quantitative idea of how large that systematic error can become if a narrow interval about that instant is chosen for the fitting. Obviously, if the measurement is not so local, i.e. the fitting interval starting at t_{trans} is wider, the systematic error will be smaller than the labelled value, since the instantaneous error decays along that interval. For large Ohnesorge numbers, the growth during the transient is qualitatively similar, but the transient is then more brief because the subdominant mode decays more quickly, as seen in our description of the dispersion relation (see figure 2).

In figure 13, the two-normal-mode analysis agrees very well with the nonlinear numerical simulation during the transient. In addition, this comparison makes evident the nonlinearities that appear for large enough amplitudes. In the most viscous case, the deviation from the linear prediction is evident almost from the beginning, because the initial amplitude chosen by Bousfield & Denn (1987) was relatively large. An accurate experimental measurement of the growth rate would be impossible with these conditions, but a two-exponential fit would allow us to measure closer to the nozzle, where the amplitude is smaller and the linearity assumption is better fulfilled.

Xing *et al.* (1996) measured the deformation amplitude through the shadow method. Their data, shown in figure 14, are suitable for growth-rate fitting. We can now interpret the initial deviation from a straight line, which we have called a rapid-growth transient, as a consequence of the initial combination of the dominant and subdominant capillary modes for pure-impulse initial conditions. The full normal-mode analysis predicts the transient well for $x \geqslant 25$. We emphasize that the only fitted data come from the purely exponential phase. The arrows mark the end of the transient, according to the labelled error level for the instantaneous growth rate relative to the theoretical one. For the first time, there is an estimate of where the purely exponential growth starts. Workers interested in measuring growth rates,

either experimentally or computationally, should take such estimates as a lower limit of amplitudes for fitting.

Concerning the departure from the theoretical curve close to the nozzle, we can only give some speculative hypotheses. Against the widely accepted assumption of purely impulsive initial conditions from piezoelectric stimulation jets, there is a non-zero deformation at $x = 0$, i.e. at the exit orifice. A possible explanation is that the nozzle orifice might not be at $x = 0$, but a few hundred micrometres upstream. This is apparently supported by the slight relative misplacement of the data from their figures 4(a) and 4(c) (the same experimental conditions but different optical set-ups). The transient predicted by tentative mixed initial conditions at $x = 0$ is plotted in figure 14. Although they match the whole transient better, a small systematic deviation suggests that this is not the correct explanation or at least, not the only one. The relaxation of the velocity profile after the jet emerges could have a role. Concerning the experimental technique, the shadow method could be difficult to apply to the beginning of the jet, owing to reflection or diffraction from the nozzle. In addition, the nozzle itself could vibrate harmonically. Small non-axisymmetric deformations could distort the signal from the shadow technique (González & García 2008). In our opinion, new experiments and simulations exploring the deformation near the nozzle are necessary to understand the exact nature of the initial conditions of capillary jets.

The dependence of the transient duration on C and k for pure-impulse initial conditions, represented in figure 15, can be easily explained thanks to our detailed description of the dependence of α_d and α_s on C and k. For small viscosity ($C < 0.1$), $\alpha_d - \alpha_s$ is maximum if $k \simeq k_{max}$. Therefore, according to (3.33), the transient time will be minimum in the interval $0.6 \lesssim k \lesssim 0.8$, taking about eight times the capillary time in dimensional units. In the limits of small k and $k \simeq k_c$, α_d and $|\alpha_s|$ are smaller and they approach each other, so the transient is significantly longer.

As viscous shear becomes important, $|\alpha_s|$ increases, specially for k not small. This is why the transient duration diminishes for k not small. Owing to the smallness of α_d, only for moderate C and very near k_c does the transient last longer. This explains why Berger noted a considerably longer transient for $k = 0.1$ than for $k = 0.9$ with $C = 0.23$. For large C, the transient is clearly shorter for k not small. Although for k small it is much larger, its duration is less important than for small viscosity because the breakup time is so large.

Figure 16, computed with (3.34), is more indicated to check experimentally the theoretical growth rate of the dominant mode, since it is an absolute error level which is fixed. The only significant change with respect to the above discussion happens for k far from k_{max}, since this criterion is less exacting when α_d is far from its maximum value. Even so, our previous discussion about the transient duration remains valid.

Let us discuss the difficulties that an experimenter has to overcome to successfully reproduce the Rayleigh dispersion curve, i.e. the growth rate of the dominant mode against the wavenumber. Even in the small-perturbation phase, he will encounter two enemies: noise and the initial transient. On the one hand, very small-amplitude perturbations are technically difficult to measure (Goedde & Yuen 1970; Taub 1976; Xing *et al.* 1996). They have to compete against noise. Noisy natural perturbations, although of small amplitude, cover the whole frequency spectrum. The most harmful, those with $k \simeq k_{max}$, grow with the maximum growth rate α_{max}. This compels the experimenter to choose a large enough initial amplitude to prevent the disturbing noise from having time to dominate over the imposed periodic perturbation. On the other hand, the initial transient makes difficult the measurement for small amplitude, as do

the nonlinear effects when the amplitude becomes large. This forces the experimenter to choose a small enough initial amplitude so that the purely exponential growth phase lasts for enough time (or distance) to make the measurement. A compromise is thus necessary. This is why it is so important to have good estimates of the interval of pure exponential growth.

For small C and $k \simeq k_{max}$, a small initial amplitude clearly stronger than the natural noise suffices, since both kinds of perturbation grow at the same rate. It is then only a matter of choosing the proper interval of amplitudes for the fitting. However, as k moves away from k_{max}, first, the noise grows more quickly than the periodic disturbance and ruins the signal-to-noise ratio; secondly, the transient is longer. For very small k or when approaching k_c, it is impossible to measure the growth rate accurately.

Thus, there is a practical lower limit for the initial amplitude in experiments to determine the growth rate. It is therefore convenient either to know a good estimate of the transient duration in order to avoid it, or to know the expected functional time dependence of the deformation during the transient so as to use all the data from the beginning, as in figure 12. Not doing so would lead to systematically wrong measurements of the growth rate.

Concerning the two-exponential fitting method to include the transient phase, it could be advantageous in two more ways. First, it could provide the growth rate of the two capillary modes, which has not been done before. Secondly, the same fitting would give us information about the initial deformation and velocity for general initial conditions. This would be useful for characterizing new stimulation devices, since it is very difficult to measure the small initial velocity perturbations of a liquid jet (Dressler 1998).

5.3. *Generality of the modal analysis*

The equations found for the transient duration and the evolution of both the surface deformation and the mean axial velocity are simple expressions in terms of the eigenvalues α_d and α_s. In principle, we have restricted our normal-mode analysis to the classical initial-value problem of an infinite viscous jet. However, the idea of expressing the evolution in terms of the two capillary modes, instead of only the most dominant mode, is general. It can be extended to slightly different physical systems that include other effects: slight aerodynamic shear, viscoelasticity, electric or magnetic forces, small spatial-instability deviation due to a small Weber number, Marangoni instability (Chakraborty 2005; Furlani 2005), swirling, etc. The dispersion relation, as well as the values of α_d and α_s, will be different in each case, but an initial transient is expected. Its duration will be given by an expression similar to the one in our analysis, provided that there are no significant changes in the normal modes. The same expressions might be generalized to systems similar to capillary jets, as hollow jets or compound jets. In fact, we have mentioned a clear case of slow-growth initial transient in numerical simulations of a compound jet with pure-deformation initial conditions (Suryo *et al.* 2006).

Frequently, the normal-mode linear analysis is taken as an auxiliary tool to validate numerical simulation codes. It may also be required in experiments, to validate a theoretical model, to test the apparatus, to find out the initial conditions, or even to accurately determine some elusive parameter of the system, such as the dynamic surface tension. A consequence of the above analysis is that it is advisable to undertake a complete normal-mode analysis, not restricted to the most dominant mode. Only in that way can the appropriate connection to the initial-value problem be established.

6. Conclusions and future work

Contrary to what was previously thought, we have demonstrated that the Rayleigh normal-mode linear analysis predicts the non-exponential growth transient that occurs in the first stages of the evolution of an infinite capillary jet subject to periodic initial perturbations. In order to establish a bi-unique correspondence between initial conditions and initial amplitudes of normal modes, it is necessary to know all roots of the dispersion relation and their respective normal modes.

There are two kinds of mode: the two already-known capillary modes, called dominant and subdominant; and an infinite set of hydrodynamic modes. In order to satisfactorily describe the initial transient, the two capillary modes are necessary when general non-recirculating initial conditions are considered. The hydrodynamic modes have a recirculating velocity field and relatively small deformation of the surface and mean axial velocity. These allow the normal-mode analysis to account for periodic recirculating initial conditions.

General non-recirculating initial conditions have been formally considered, including the arbitrary temporal phase between deformation and mean axial velocity. The two particular sets of initial conditions more usual in the literature have been discussed in detail: pure deformation and pure impulse. When the initial disturbance is a pure deformation of the surface, the amplitude of the deformation grows more slowly than the dominant mode during the transient (slow-growth transient). Conversely, when the initial disturbance is purely impulsive, as expected in acoustic stimulation, the disturbance grows more rapidly than the dominant mode (rapid-growth transient). In both cases, the amplitudes of the two capillary normal modes can be readily obtained from the initial amplitude of the perturbation. In particular, the initial velocity perturbation of an acoustically stimulated jet can be deduced from the subsequent evolution of the surface-deformation amplitude.

The normal-mode linear analysis accurately predicts the same kind of initial transient as observed in previous computations and our own one-dimensional numerical simulations of the initial-value problem. The normal-mode analysis quantitatively agrees with a previous experiment in a wide range of amplitudes. However, neither the normal-mode analysis nor the nonlinear numerical simulation with pure-impulse initial conditions can account for the non-zero initial deformation amplitude measured in that experiment. New experiments measuring the early evolution would be interesting in order to find whether the actual initial conditions of acoustically stimulated jets are purely impulsive, as thought until now.

A simple but accurate estimate of the the initial-transient duration has been derived for purely impulsive initial conditions. For small Ohnesorge numbers, the transient duration significantly increases for wavenumbers far from the maximum-growth wavenumber. When the Ohnesorge number increases, the transient becomes shorter and shorter for moderate or near-to-unit wavenumbers; its relative significance in the evolution diminishes as compared to the increasing breakup time.

Knowing the initial transient duration will be useful for experimenters interested in accurately measuring the growth rate of the dominant mode, as it marks the beginning of the exponential growth phase, suitable for data fitting. In particular, special care is necessary when interested in low Ohnesorge numbers and wavenumbers far from the maximum-growth value, as the exponential growth phase could disappear. In order to delimit the end of the interval for measuring the growth rate, a nonlinear perturbation analysis is under way.

The analysis presented is quite general, in the sense that the derived expressions are in terms of the roots of the dispersion relation. Therefore, in many cases, those expressions can readily be extended to account for other effects apart from surface tension and viscous shear, provided that the eigenvalues of the corresponding dispersion relation for the necessary normal modes are computed. Workers interested in the linear analysis of capillary jets and other related physical systems should consider all roots in their dispersion relation, including those that are apparently less significant. More than one mode is necessary to describe the initial transient of the initial-value problem.

In the past, the normal-mode linear analysis has proved to be useful for studying capillary jets. No other more complex tools have given such a simple and intuitive insight into the evolution of the jet. Although its validity for describing the early growth of the applied disturbance has been under suspicion, it is now clear that this was not warranted. Moreover, the connection established here between the normal-mode analysis and the initial conditions will help to solve some basic questions not satisfactorily answered until now. A direct practical application is the formulation of theoretical transfer functions to relate the initial amplitude of the dominant mode to the measurable quantity that controls the stimulation, which we shall discuss in future work.

We are grateful to Dr Nasser Ashgriz and Dr Farzad Mashayek for providing some data used in figures 10, 11 and 12. We also thank Dr Pierre Atten and Dr Antonio Castellanos for helpful discussions.

This research was supported by the Spanish Ministerio de Ciencia y Tecnología, under contract FIS2006-03645; and by the Junta de Andalucía, under contract FQM-421.

REFERENCES

Alakoç, U., Megaridis, C. M., McNallan, M. & Wallace, D. B. 2004 Dynamic surface tension measurements with submillisecond resolution using a capillary-jet instability technique. *J. Colloid Interface Sci.* **276**, 379–391.

Apfel, R. E., Tian, Y., Jankovsky, J., Shi, T., Chen, X., Holt, R. G., Trinh, E., Croonquist, A., Thornton, K. C., Sacco, Jr, A., Coleman, C., Leslie, F. W. & Matthiesen, D. H. 1997 Free oscillations and surfactant studies of superdeformed drops in microgravity. *Phys. Rev. Lett.* **78** (10), 1912–1915.

Ashgriz, N. & Mashayek, F. 1995 Temporal analysis of capillary jet breakup. *J. Fluid Mech.* **291**, 163–190.

Basaran, O. A. 2002 Small-scale free surface flows with breakup: drop formation and emerging applications. *AIChE J.* **48**, 1842–1848.

Basaran, O. A. & Depaoli, D. W. 1994 Nonlinear oscillations of pendant drops. *Phys. Fluids* **6** (9), 2923–2943.

Battal, T., Bain, C. D., Weiss, M. & Darton, R. C. 2003 Surfactant adsorption and Marangoni flow in liquid jets I. Experiments. *J. Colloid Interface Sci.* **263**, 250–260.

Bellizia, G., Megaridis, C. M., McNallan, M. & Wallace, D. B. 2002 A capillary-jet instability method for measuring dynamic surface tension of liquid metals. *Proc. R. Soc. Lond.* A **459**, 2195–2214.

Berger, S. A. 1988 Initial-value stability analysis of a liquid jet. *SIAM J. Appl. Maths* **48**, 973–991.

Bogy, D. B. 1978 Use of one-dimensional Cosserat theory to study instability in a viscous liquid jet. *Phys. Fluids* **21** (2), 190–197.

Bousfield, D. W. & Denn, M. M. 1987 Jet breakup enhanced by an initial pulse. *Chem. Engng Commun.* **53**, 61–68.

Chakraborty, S. 2005 Analytical investigations on breakup of viscous liquid droplets on surface tension modulation during welding metal transfer. *Appl. Phys. Lett.* **86**, 174104.

Chandrasekhar, S. 1961 *Hydrodynamic and Hydromagnetic Stability*. Clarendon.

Chaudhary, K. C. & Redekopp, L. G. 1980 The nonlinear capillary instability of a liquid jet. Part 1. Theory. *J. Fluid Mech.* **96**, 257–274.

Chen, A. U., Notz, P. K. & Basaran, O. A. 2002 Computational and experimental analysis of pinch-off and scaling. *Phys. Rev. Lett.* **17** (88), 174501.

Chuech, S. G. & Yan, M.-M. 2006 Application of the TVD scheme to the nonlinear instability analysis of a capillary jet. *Intl J. Numer. Meth. Fluids* **52**, 1159–1174.

Collantes, G. O., Yariv, E. & Frankel, I. 2003 Effects of solute mass transfer on the stability of capillary jets. *J. Fluid Mech.* **474**, 95–115.

Collicott, S. H., Zhang, S. & Schneider, S. P. 1994 Quantitative liquid jet instability measurement system using asymmetric magnification and digital image processing. *Exps. Fluids* **16**, 345–348.

Donnelly, R. J. & Glaberson, W. 1966 Experiments on the capillary instability of a liquid jet. *Proc. R. Soc. Lond.* **290**, 547–556.

Dressler, J. L. 1998 High-order azimuthal instabilities on a cylindrical liquid jet driven by temporal and spatial perturbations. *Phys. Fluids* **10** (9), 2212–2227.

Eggers, J. 1997 Nonlinear dynamics and breakup of free-surface flows. *Rev. Mod. Phys.* **69**, 865–929.

Eggers, J. & Dupont, T. F. 1994 Drop formation in a one-dimensional approximation of the Navier–Stokes equation. *J. Fluid Mech.* **262**, 205–221.

Furlani, E. P. 2005 Temporal instability of viscous liquid microjets with spatially varying surface tension. *J. Phys.* A: *Math. Gen.* **38**, 263–276.

García, F. J. 1998 Aplicación de modelos unidimensionales a la dinámica de columnas líquidas con y sin campo eléctrico. PhD thesis, Universidad de Sevilla, Seville, Spain.

García, F. J. & Castellanos, A. 1994 One-dimensional models for slender axisymmetric viscous liquid jets. *Phys. Fluids* **6** (8), 2676–2689.

García, F. J. & Castellanos, A. 1999 3-D and 1-D dynamics of slender liquid jets: linear analysis with electric field and accuracy of 1-D models near the breakup. In *1999 Conference on Electrical Insulation and Dielectric Phenomena*, pp. 346–349.

García, F. J., Castellanos, A., Atten, P. & Barbet, B. 2000 Nonlinear one-dimensional modelling of the deformation and break-up of a conducting liquid jet under intermittent EHD stimulation. In *Second Intl Workshop on EHD and Breakdown*, pp. 158–161. Grenoble, France.

Goedde, E. F. & Yuen, M. C. 1970 Experiments on liquid jet instability. *J. Fluid Mech.* **40**, 495–511.

González, H. & García, F. J. 2008 The measurement of growth rates in capillary jets. *J. Fluid Mech.* Submitted.

Green, A. E. 1976 On the nonlinear behavior of fluid jets. *Intl J. Engng Sci.* **14**, 49–63.

Gresho, P. M., Lee, R. L. & Sani, R. L. 1980 On the time-dependent solution of the incompressible Navier–Stokes equations in two and three dimensions. In *Recent Advances in Numerical Methods in Fluids* (ed. C. Taylor & K. Morgan), vol. 1, chap. 2, pp. 27–79. Pineridge, Swansea, UK.

Grossmann, S. & Müller, A. 1984 Instabilities and decay rates of charged viscous liquid jets. *Z. Phys.* B **57**, 161–173.

Hansson, B. A. M. & Hertz, H. M. 2004 Liquid-jet laser-plasma extreme ultraviolet sources: from droplets to filaments. *J. Phys.* D: *Appl. Phys.* **37**, 3233–3243.

Jatzkowski, T. & Modigell, M. 2005 Experiments on axisymmetric oscillating water jets: absorption of ammonia in presence of *n*-pentanol. *Colloids Surfaces* A: *Physicochem. Engng Aspects* **255**, 41–53.

Kalaaji, A., Lopez, B., Attané, P. & Soucemarianadin, A. 2003 Breakup length of forced liquid jets. *Phys. Fluids* **15** (9), 2469–2479.

Keller, J. B., Rubinow, S. I. & Tu, Y. O. 1973 Spatial instability of a jet. *Phys. Fluids* **16** (12), 2052–2055.

Le, H. P. 1998 Progress and trends in ink-jet printing technology. *J. Imaging Sci. Technol.* **42**, 49–62.

Lee, H. C. 1974 Drop formation in a liquid jet. *IBM J. Res. Develop.* **18**, 364–369.

Levich, V. G. 1962 *Physicochemical Hydrodynamics*. Prentice–Hall.

Lin, S. P. 2003 *Breakup of Liquid Sheets and Jets*. Cambridge University Press.

Mansour, N. N. & Lundgren, T. S. 1990 Satellite formation in capillary jet breakup. *Phys. Fluids* A **2**(7), 1141–1144.

Nicolás, J. A. & Vega, J. M. 2000 Linear oscillations of axisymmetric viscous liquid bridges. *Z. Angew. Math. Phys.* **51**, 701–731.

Pan, Y. & Suga, K. 2006 A numerical study on the breakup process of laminar liquid jets into a gas. *Phys. Fluids* **18** (5), 052101.

Plateau, J. 1873 *Statique Expérimentale et Théorique des Liquides Soumis aux Seules Forces Moléculaires*. Gauthier Villars, Paris.

Ramos, A., García, F. J. & Valverde, J. M. 1999 On the breakup of slender liquid bridges: experiments and a 1-D numerical analysis. *Eur. J. Mech.* B/*Fluids* **18**, 649–658.

Rayleigh, Lord 1878 On the instability of jets. *Proc. Lond. Math. Soc.* **10**, 4–13.

Rayleigh, Lord 1892 On the instability of a cylinder of viscous liquid under capillary forces. *Philos. Mag.* **34**, 145–154.

Rayleigh, Lord 1945 *The Theory of Sound*, 2nd edn. Dover.

Ronay, M. 1978*a* Determination of the dynamic surface tension of inks from the capillary instability of jets. *J. Colloid Interface Sci.* **66**, 55–67.

Ronay, M. 1978*b* Determination of the dynamic surface tension of liquids from the instability of excited capillary jets and from the oscillation frequency of drops issued from such jets. *Proc. R. Soc. Lond.* A **361**, 181–206.

Rutland, D. F. & Jameson, G. J. 1970 Theoretical predictions of the sizes of drops in the breakup of capillary jets. *Chem. Engng Sci.* **25**, 1689–1698.

Saroka, M., Guo, Y. & Ashgriz, N. 2001 Nonlinear instability of an evaporating capillary jet. *AIAA J.* **39**, 1728–1734.

Sellens, R. W. 1992 A onedimensional numerical model of capillary instability. *Atom. Sprays* **2**, 239–251.

Shapiro, H. M. 2003 *Practical Flow Cytometry*, 4th edn. Wiley–Liss, Hoboken.

Strang, G. & Fix, G. J. 1973 *An Analysis of the Finite Element Method*. Prentice–Hall.

Suryo, R., Doshi, P. & Basaran, O. A. 2006 Nonlinear dynamics and breakup of compound jets. *Phys. Fluids* **18** (8), 082107.

Sweet, R. G. 1965 High frequency recording with electrostatically deflected ink jets. *Rev. Sci. Instrum.* **36**, 131–136.

Taub, H. 1976 Investigation of nonlinear waves on liquid jets. *Phys. Fluids* **19** (8), 1124–1129.

Torpey, P. A. 1989 A nonlinear theory for describing the propagation of disturbances on a capillary jet. *Phys. Fluids* A **1** (4), 661–671.

Weber, C. 1931 Zum Zerfall eines Flüssigkeitsstrahles. *Z. Angew. Math. Mech.* **11**, 136–154.

Weiss, M., Darton, R. C., Battal, T. & Bain, C. D. 2004 Surfactant adsorption and Marangoni flow in liquid jets. 2. Modeling. *Indust. Engng Chem. Res.* **43**, 5203–5220.

Wetsel, G. C. 1980 Capillary oscillations on liquid jets. *J. Appl. Phys.* **51**, 3586–3592.

Wilkes, E. D., Phillips, S. D. & Basaran, O. A. 1999 Computational and experimental analysis of dynamics of drop formation. *Phys. Fluids* **11** (12), 3577–3598.

Xing, J. H., Boguslawski, A., Soucemarianadin, A., Atten, P. & Attané, P. 1996 Experimental investigation of capillary instability: results on jet stimulated by pressure modulations. *Exps. Fluids* **20**, 302–313.

Yuen, M. 1968 Nonlinear stability of a liquid jet. *J. Fluid Mech.* **33**, 151–163.

Zhang, X., Padgett, R. S. & Basaran, O. A. 1996 Nonlinear deformation and breakup of stretching liquid bridges. *J. Fluid Mech.* **329**, 207–245.